

ALMA MATER STUDIORUM - UNIVERSITÀ DI BOLOGNA
CAMPUS DI CESENA
SCUOLA DI INGEGNERIA E ARCHITETTURA
CORSO DI LAUREA MAGISTRALE IN INGEGNERIA BIOMEDICA

Development of an instrumented customizable total knee prosthesis for experimental tests

Elaborato in
MECCANICA DEI TESSUTI BIOLOGICI LM

Relatore
Prof. Luca Cristofolini

Presentata da
Alessandra Ventresca

Correlatori
Prof. Bernardo Innocenti
Silvia Pianigiani, PhD

I sessione
anno accademico 2015/2016

“L’aquilone, per volare,
ha bisogno del vento contrario”

Contents

Prefazione	1
Abstract	4
1 Introduction	7
1.1 The knee	7
1.1.1 Anatomy	7
1.1.2 Biomechanics	10
1.2 Total Knee Arthroplasty	12
1.2.1 Reasons of surgery	12
1.2.2 Designs	13
1.3 Instrumented knee implants: state of the art	16
2 Aim of the thesis	23
3 Materials and methods	25
3.1 Analytical study	26
3.1.1 Tibio-femoral joint	28
3.1.2 Patello-femoral joint	31
3.2 Design	32
3.2.1 Force sensing	33
3.2.1.1 Instrumented tibial tray	35
3.2.1.1.1 First design	36
3.2.1.1.2 Second design	38
3.2.1.2 Instrumented patella	40
3.2.2 Position sensing	41
3.3 Manufacturing	45
3.3.1 Six-axis load cell	45
3.3.2 Three-layers piezo-resistive position sensor	48
4 Testing and results	55

5 Discussion and future perspectives	64
6 Conclusions	67
7 Bibliography	69
8 Appendix	74

Prefazione

La protesi totale di ginocchio (PTG) ha rivoluzionato la vita di milioni di pazienti e rappresenta il trattamento più efficiente nei casi di osteoartrite. Circa 700,000 procedure vengono effettuate ogni anno negli USA e questo numero è destinato ad aumentare. Inoltre, l'incremento della aspettativa di vita ha abbassato l'età media del paziente tipo, che richiede quindi una protesi più longeva e performante. Ad oggi infatti, la durata media di una protesi è di circa 10-15 anni, dopo i quali essa fallisce ed è necessaria una procedura di revisione spesso costosa e molto invasiva. Inoltre, spesso capita che, nonostante le immagini radiografiche non indichino alcun segno di fallimento, il paziente si dichiari insoddisfatto.

Per migliorare il design delle protesi e soddisfare le esigenze dei pazienti, è necessaria una profonda conoscenza della biomeccanica del ginocchio. A tale scopo, i modelli numerici (analisi del corpo rigido e analisi agli elementi finiti) rappresentano un mezzo molto utilizzato dai ricercatori, per simulare ed analizzare varie configurazioni del ginocchio sano o protesizzato in modo non invasivo, veloce ed economico. In questo campo sono stati fatti numerosi progressi, tuttavia la modellazione numerica rimane un metodo molto problematico in quanto i modelli sono fortemente dipendenti da input esterni e hanno bisogno di essere validati sperimentalmente. Per superare l'incertezze dei modelli numerici, il ginocchio viene studiato anche attraverso metodi sperimentali. Un esempio è rappresentato dal Tekscan, sensore di pressione che misura dinamicamente l'area e la pressione di contatto tra due oggetti in articolazione: esso viene spesso utilizzato nei test sperimentali sulle protesi di ginocchio per ricavare dati cinetici e cinematici. Tuttavia esso presenta numerose limitazioni: è fragile, costoso ed ha una risoluzione non ottimale. Un'altra alternativa sperimentale sono le protesi strumentate: prendendo spunto dai primi sistemi realizzati per l'anca, il primo prototipo per il ginocchio risale al 1996, quando Kaufman et al. misurarono la forza tibiofemorale assiale e il suo centro di pressione. Successivamente, D'Lima et al. hanno aggiunto un sistema telemetrizzato per la trasmissione dei dati, e realizzato un secondo prototipo che misura sei componenti di forza e momento. Parallelamente, un altro gruppo di ricerca, guidato da Bergmann, ha messo a punto un prototipo molto simile di protesi strumentata. In entrambi i casi, i carichi registrati vengono integrati con dati cinematici simultaneamente acquisiti: nel primo caso, con un sistema di imaging fluoroscopico, nel secondo caso tramite gait analysis. I dati cinematici vengono combinati matematicamente con quelli cinetici in

postprocessing per dividere le componenti di forza tibiofemorale mediale e laterale. Questi dispositivi sono stati testati in vivo ed in vitro, permettono di misurare le forze interne del ginocchio durante numerose attività, e attualmente vengono presi come standard di riferimento per i carichi interni del ginocchio.

Lo scopo della tesi è stato quello di progettare e realizzare un nuovo prototipo di protesi strumentata in grado di misurare la cinetica e la cinematica di differenti intercambiabili design di protesi durante prove sperimentali all'interno di un laboratorio di ricerca, su simulatore robotico di ginocchio. A differenza dei prototipi precedenti quindi, esso non è rivolto ad applicazioni industriali, ma puramente di ricerca.

Dopo un accurato studio della letteratura, ed uno studio analitico preliminare, il progetto è stato realizzato ispirandosi ai prototipi di D'Lima e Bergmann, quindi il sensing della forza e della cinematica sono stati trattati separatamente. Il file CAD di una protesi commerciale è stato modificato, compatibilmente con le possibilità realizzative del laboratorio meccanico del dipartimento BEAMS dell'ULB (Université Libre de Bruxelles): lo stelo tibiale cilindrico è stato estensimetrato, diventando l'elemento sensibile di una cella di carico, fissata al simulatore robotico da un lato, e collegata all'inserito tibiale dall'altro, mediante un piatto tibiale. Il dispositivo è completamente modulare quindi, una volta calibrata la cella di carico e fissata sul simulatore, è possibile testare differenti design di protesi semplicemente cambiando il piatto tibiale superiore. Inoltre, per la prima volta è stata considerata l'articolazione patello-femorale, fino ad ora sempre trascurata dalle protesi strumentate. A partire da un file CAD di un inserto patellare, è stato disegnato un sistema che funge non solo da blocco di montaggio sul simulatore robotico, ma anche da sostegno per l'elemento sensibile della cella di carico, che è identico a quello dell'articolazione tibiofemorale ed è posizionato sul retro dell'inserto patellare.

Per quanto riguarda i dati cinematici, è stato progettato, realizzato e testato un sensore piezoelettrico a tre strati, che rappresenta un metodo innovativo alternativo al Tekscan e ad altri metodi poco accurati ed invasivi fino ad ora utilizzati. Il test pilota ha mostrato una risposta positiva del sensore, il quale ha seguito dinamicamente i movimenti della protesi. Nello studio dell'articolazione tibiofemorale questi dati sono fondamentali per suddividere il contributo di forza mediale da quello laterale.

A differenza delle protesi strumentate realizzate fino ad ora, i dati cinetici e cinematici potranno essere acquisiti e combinati attraverso un unico sistema di acquisizione, il quale può fornire in real-time la percentuale di distribuzione della forza tibio-femorale nelle componenti mediale e laterale

senza bisogno di elaborazioni successive. Inoltre il dispositivo è estremamente economico, non altera la cinematica delle protesi di ginocchio, ed è facilmente adattabile a qualsiasi simulatore di ginocchio.

Abstract

Total knee arthroplasty (TKA) has revolutionized the life of millions of patients and it is the most efficient treatment in cases of osteoarthritis. About 700,000 procedures are performed each year in the USA and this number is expected to increase. In addition, the increase in life expectancy has lowered the average age of the patient, which then requires a more enduring and performing prosthesis. Currently, in fact, the average survival rate of a prosthesis is about 10-15 years: after the failure of the implant, a very expensive and invasive revision procedure is often necessary. In addition, it often happens that, despite the X-rays images do not indicate any sign of failure, the patient declares himself dissatisfied.

To improve the design of implants and satisfying the patient's needs, a deep understanding of the knee Biomechanics is needed. To this end, numerical models (rigid body analysis and finite elements modeling) are often used by researchers to simulate and analyze various configurations of prosthetic or healthy knee non-invasively, quickly and inexpensively. Much progress has been made in this area, however the numerical modelling remains a very challenging field because the models are highly dependent on external inputs and need to be validated experimentally.

To overcome the uncertainties of numerical models, the knee is also studied through experimental methods. An example is the Tekscan system, pressure sensor that measures dynamically areas and contact pressure between two articulating objects in: it is often used in experimental tests on the knee to derive kinematic and kinetic data.

However it has several limitations: it is fragile, expensive and has a non-optimal resolution.

Another experimental alternative is represented by instrumented orthopedic implants: taking cues from early systems made for the hip, the first prototype for the knee goes back to 1996, when Kaufman et al. measured the tibial-femoral axial force and its center of pressure (COP). Then, D'Lima et al., added a telemetry system for data transmission, and realized a second prototype that enabled the measurement of six force and moment components.

In parallel, another research group, driven by Bergmann, manufactured a similar device of instrumented tibial tray. In both cases the measured loads must be integrated with kinematic data registered simultaneously: in the first case, with a dual fluoroscopic imaging system, in the second case by gait analysis. Kinematic data are combined mathematically with kinetic ones in postprocessing to divide the medial and lateral tibiofemoral joint force components. These devices

have been tested in vivo and in vitro, to measure the internal forces of the knee during many activities, and currently are taken as reference standards for internal loads of the knee.

The aim of the thesis was to design and manufacture a new prototype of instrumented implant, able to measure kinetic and kinematic data of different interchangeable designs of prosthesis during experiments tests within a research laboratory, on robotic knee simulator. Unlike previous prototypes it is not aimed for industrial applications, but purely focusing on research.

After a careful study of the literature, and a preliminary analytic study, the project was inspired by the prototypes of D'Lima and Bergmann, then the force sensing and kinematics sensing were treated separately.

The CAD file of a commercially available prosthesis was modified, depending on the possibilities of mechanical laboratory of the Department BEAMS of ULB (Université Libre de Bruxelles): cylindrical tibial stem was covered by strain gauges, becoming the sensing element of a load cell, mounted on robotic Simulator at one side, and connected to the tibial insert on the other, by means of an interchangeable tibial plateau. The device is completely modular, so once calibrated the load cell and mounted on the knee simulator, it can test different designs of prostheses just by changing the upper tibial plateau.

Also, for the first time it was considered the patellofemoral joint, until now always neglected by instrumented implants. Starting from a CAD file of a patellar insert was designed a structure that works as mounting block on robotic knee simulator, but also as support for the sensing element of the load cell, which is identical to that of the tibiofemoral joint and is located at the back of the patellar insert.

As for the kinematic data, was designed, manufactured and tested a three-layer piezoelectric sensor, which is an innovative alternative to Tekscan system and other inaccurate and invasive methods used until now. The pilot test showed a positive response of the sensor, which dynamically followed the movements of the prosthesis. In the case of tibio-femoral joint study, kinematics data serve to divide the medial and lateral tibiofemoral joint force component.

Unlike instrumented implants performed until now, kinetic and kinematic data can be captured and combined through an unique data acquisition platform, which can provide real-time tibio-femoral force distribution percentage in medial and lateral components without the need for subsequent processing. Also the device is extremely cheap, does not alter the kinematics of the knee, and is easily adaptable to any knee Simulator.

1. Introduction

1.1 The knee

1.1.1 Anatomy

The knee is a multi-articular joint of the lower limbs that ensures the stability and the relative motion between the lower and the upper leg. It is considered as the most complex articulation of human body, not only because of its anatomy and geometry, but also for its biomechanics.

The knee is an assembly of three bones: femur, tibia and patella. They articulate making two joints working at the same time: the tibiofemoral (TF) joint, between the distal femur and the proximal tibia and the patello-femoral (PF) joint between the femoral trochlear groove and the patella. Also fibula bone is included, but only to connect the soft tissues between the lower and the upper leg.

The bony architecture of the knee contributes to its stability, along with static and dynamic restraints of some soft tissues: ligaments, capsule, menisci, tendons and musculature crossing the joint. (Fig.1)

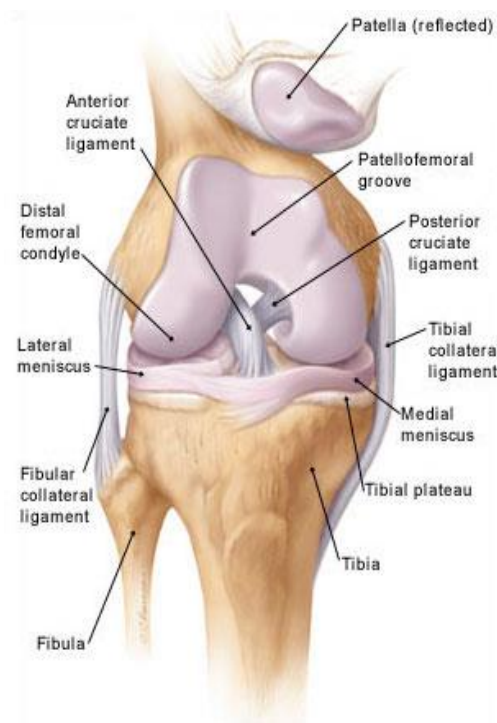


Fig.1: Open healthy knee in a partial flexion of the joint.

The femur is the longest bone of the human body, connecting the hip and the knee joints. The proximal extremity is composed by the head, the neck and the greater and the lesser trochanters, the distal extremity splits in two condyles that articulates with the corresponding tibial plateaus. So, the tibiofemoral joint is comprised of two condyloid articulations: the medial and the lateral one. The condyles are joined proximally by the femoral trochlear groove (patellar groove) that interacts with the kneecap bone, forming the patello-femoral joint. Simplistically, both the femoral condyles are cam-shaped in lateral profile, but they have different radius of curvature. The lateral condyle of the femur is smaller than the medial one, both in the antero-posterior (AP) and proximo-distal directions: this contributes to the valgus and AP alignment of the knee. (Fig.2)

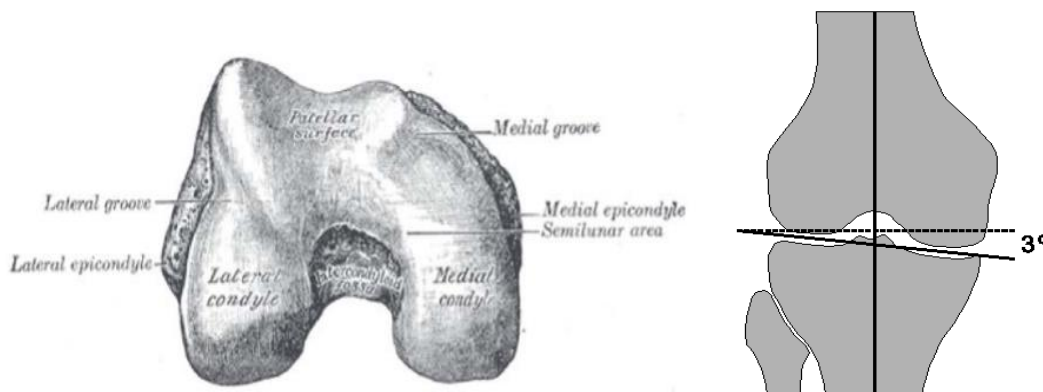


Fig.2: Inferior view of the right femoral distal epiphysis (left) and valgus alignment of the knee (right).

The proximal tibia is separated by the intercondylar eminence into two asymmetrical compartments: an oval, concave medial plateau, and a circular, convex lateral plateau. Observing the median section of the proximal tibia, it is possible to note that it has a posterior slope. (Fig.3)

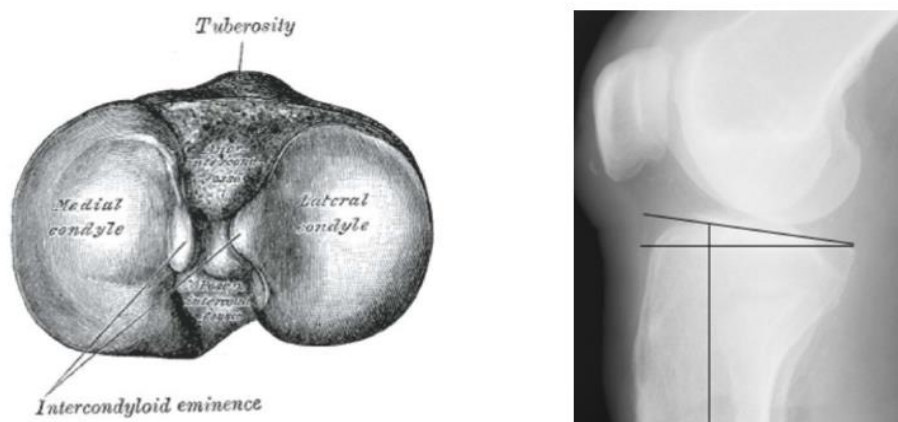


Fig.3: Superior view of the right tibial proximal epiphysis (left) and particular of the tibial posterior slope from a lateral view (right).

The patellofemoral articulation is a sellar joint between the femoral trochlear groove and patella, also known as the kneecap or kneecap, that is the largest sesamoid bone in the body, triangular in shape. (Fig.4) It lies parallel to the coronal plane of the femur, incorporated in the quadriceps tendon insertion (patellar ligament), with the apex facing downwards. The patello-femoral joint is important to knee stability primarily through its role in the extensor mechanism. The kneecap plays two important roles for the stability of the knee: it increases the mechanical advantage of the extensor muscles by increasing the moment arm of quadriceps force, and allows a better distribution of compressive forces on the femur by increasing the contact area between the patellar tendon and femur.

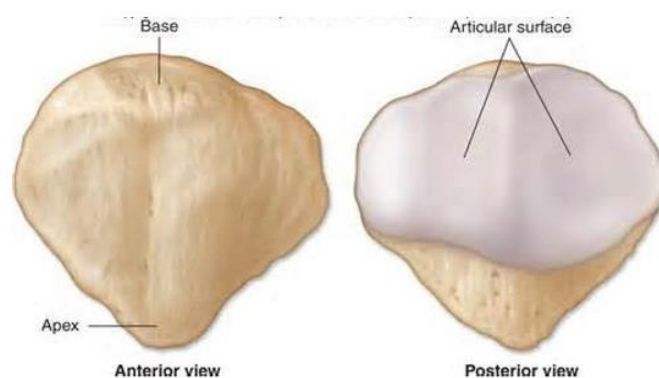


Fig.4: Anterior and posterior view of patella.

Each bone of the knee is covered by a thin layer of hyaline cartilage in the contact surfaces of the joint. The cartilage protects the underlying bone from damages and reduces the friction coefficient of the joint.

The distal femur and the proximal tibia are connected by the collateral (medial collateral ligament (MCL), lateral collateral ligament (LCL)) and the cruciate ligaments (anterior cruciate ligament (ACL), posterior cruciate ligament (PCL)), that are primary passive stabilisers against varus– valgus rotation as well as internal and external rotation. The patellar ligament connects the patellar apex to tibial tuberosity giving stability to the joint.

The menisci, two semi-lunar fibrocartilagineous pads, are located between the femoral condyles and the tibial plateaus. Besides the knee loads, they aid the joint lubrication spreading a fresh film of synovial fluid. Another important function is to distribute the forces and to reduce stresses on the structures of the joint during knee movements. ^[1,2]

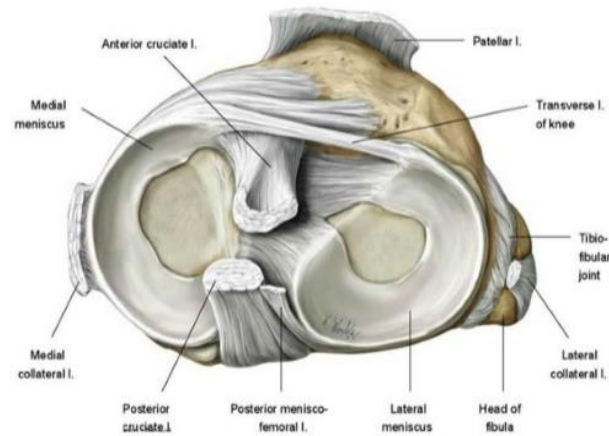


Fig.5: Head of the tibia, superior view; menisci and ligaments inserts can be seen.

1.1.2 Biomechanics

The main roles of the knee are to allow locomotion requiring minimum energy from muscles and giving stability, and to transmit, absorb and redistribute forces caused during the activities of daily life; it also acts as a pivot between the two longest bones of the human body, the femur and the tibia.

The complexity of knee joint behaviour is due to the interaction between three factors:

- Static stability – geometry and anatomy of the joint surface
- active stability – muscle contraction
- passive stability – ligaments, menisci and retinacula.

The kinematics of the knee joint is described through six degrees of freedom (three rotations and three translations) in a clinical joint coordinate system (Fig.6).

A simplified description of the knee is that it acts as a hinge in the sagittal plane. In fact the primary motion of the TF joint is the flexion-extension (FE) rotation about the epicondylar femoral axis, where it has a wide range of motion: starting from full-extension (0°), in which the tibial axis is aligned with the femoral axis, the TF joint can reach up to 160° of flexion. Also a medio-lateral (ML) translation occurs along epicondylar femoral axis. As the knee extends from 30° to 0° flexion the tibia externally rotates by up to 30° : this motion, called internal-external (IE) rotation, occurs around tibial long axis together with Joint distraction.

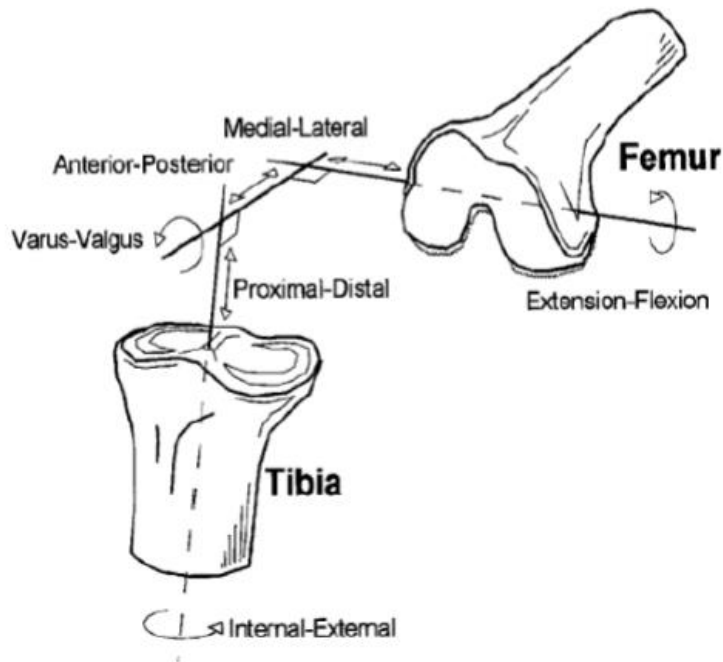


Fig.6: The six degrees of motion of the human knee joint.

Anterior-posterior translation and varus-valgus (or adduction-abduction) rotation occur along and about a floating axis, which is perpendicular to both femoral epicondylar and tibial long axes. [3] There are two mechanisms in the TF joint to take in account during the flexion-extension. First, as the knee flexes, contact moves posteriorly towards the posterior meniscal horns (roll-back) and tibial rotation occurs; however, the tibial plateaus are asymmetric (the medial plateau is more concave) so the A-P translation in the lateral side is greater than in the medial side, where the centre of contact remains almost constant. This second mechanism is the medial pivoting. (Fig.7)

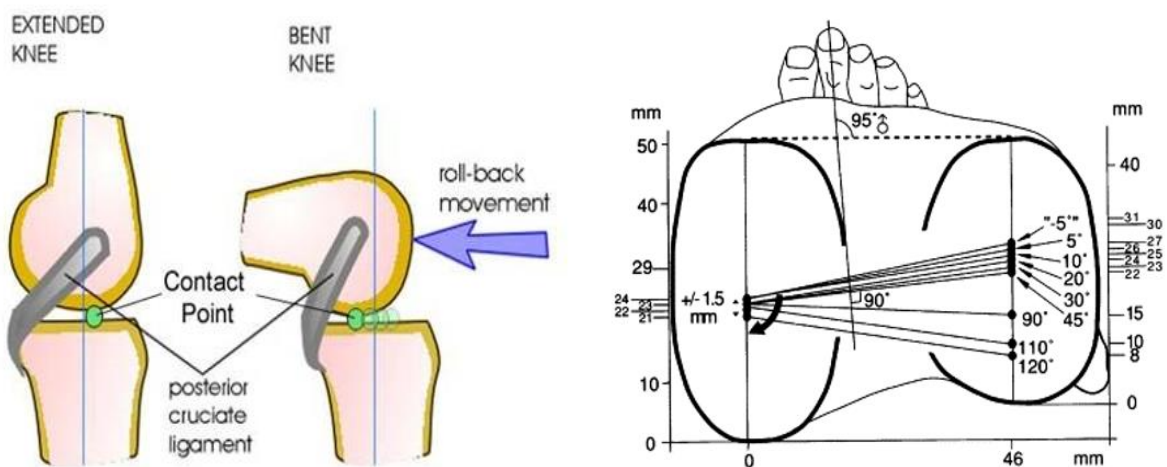


Fig.7: Roll-back mechanism (left) and medial pivoting (right).

At full TF joint extension the PF joint contact occurs at the distal end of the patella. During the flexion motion, the patella engages into the femoral trochlear groove: the contact area increases and moves proximally, by spreading the ever increasing PF joint reaction force over a larger area. This mechanism controls the magnitude of loads in the PF joint. [3]

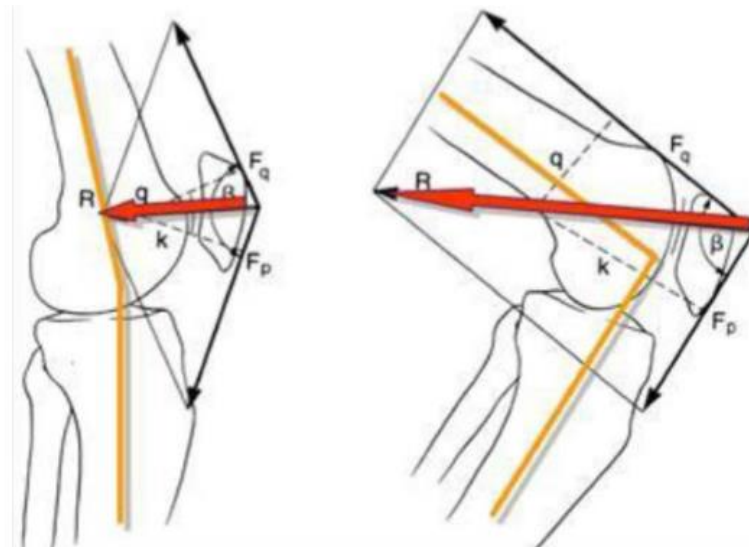


Fig.8: Patello-femoral reaction force in full extension (left) and mid-flexion (right).

1.2 Total knee arthroplasty (TKA)

1.2.1 Reasons of surgery

The knee is one of the most stressed joints as each day is subjected to a large number of load cycles, which varies depending on the level of activity of the subject. Furthermore the forces acting on the articulating surfaces of the joint are very high (they may exceed 3-4 times the body weight (BW) [4]): they are the result of outside forces, such as the reaction force on the ground, and internal forces such as those that guarantee posture and mobility.

Disease or injury can disrupt the physiological conditions of the knee, so the joint is no longer able to sustain the high daily loads, resulting in pain, muscle weakness and reduced function.

The most common cause of chronic knee pain and disability is arthritis. Although there are many types of arthritis, most knee pain is caused by just three types: osteoarthritis, rheumatoid arthritis, and post-traumatic arthritis.

Osteoarthritis (OA) usually occurs in people 50 years of age and older, but may occur in younger

people too, and it is due to hereditary, mechanical or metabolic reasons. (Fig.9)

In rheumatoid arthritis (RA) the synovial membrane that surrounds the joint becomes inflamed and thickened. This chronic inflammation can damage the cartilage, not only in the knee, but also in other joints. A serious knee injury can cause a post-traumatic arthritis: bone fractures or meniscal tears or knee ligament injuries may damage the articular cartilage over time. [2] Because of the arthritis, the cartilage that cushions the bones of the knee softens and wears away, so the bones rub against one another, causing knee pain and stiffness and reduction of mobility. When non-invasive drug therapies are not sufficient to improve the patient's condition, a knee prosthesis becomes necessary. Nowadays the market offers many solutions of knee prosthesis, available in different sizes, with the aim to satisfy the different pathological conditions and needs of patients.

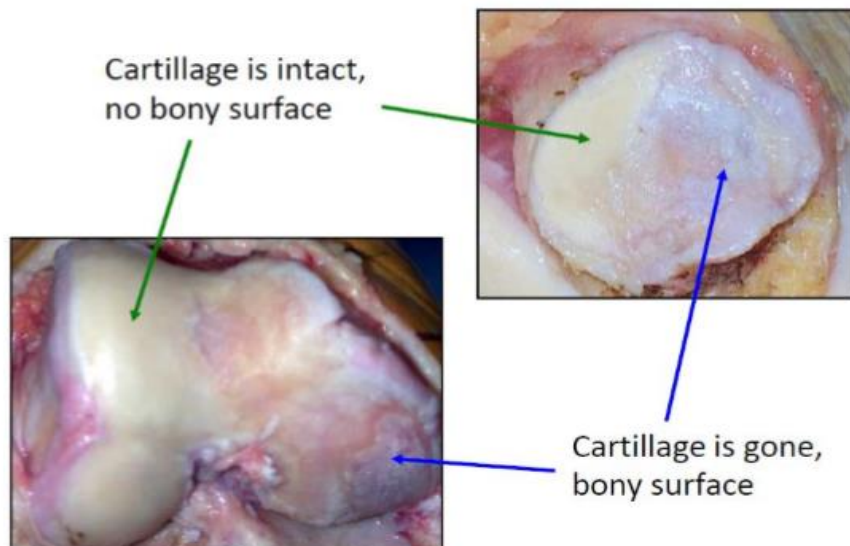


Fig.9: Knee affected by osteoarthritis.

1.2.2 Designs

The knee replacement is a procedure where damaged cartilage and the underlying bone of the knee are replaced by artificial implants, and therefore only patient with sufficient cartilage damage in at least one of the three compartments (medial, lateral, and patello-femoral) should be considered as candidate for surgery. [5]

Depending on the number of replaced compartments, knee prostheses are divided into mono-, bi- or tri-compartmental, but total knee arthroplasty (TKA) prosthesis, in which all the compartments are resurfaced, is the most widely used mainly in cases of bilateral osteoarthritis.

TKA is composed of four elements (Fig.10):

1. Femoral component: it is usually made of metal (CoCr or stainless steel) and curves up around the end of the distal femur. It can be fixed to the bone by pegs or intramedullary systems.
2. Tibial tray: it is a flat metal (CoCr alloy or Ti) platform that resurfaces the proximal tibia. For additional stability it has a stem that inserts into the center of the tibial bone.
3. Tibial insert: it is a cushion of ultra-high-molecular-weight-polyethylene (UHMWPE) mounted on the tibial tray that acts as a link between tibial and femoral components.
4. Patellar component: it is a dome-shaped UHMWPE button that resurfaces the posterior side of patella bone.

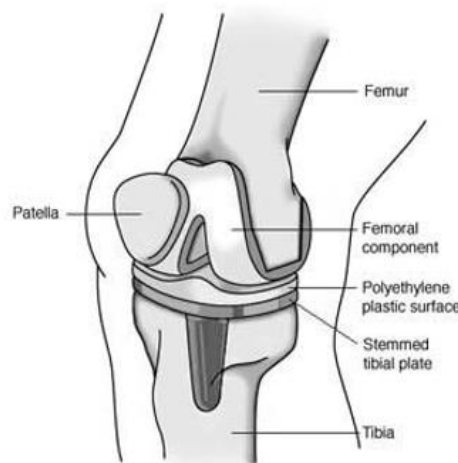


Fig.10: Knee implant components.

As has been mentioned above, there are several TKA solutions on the market, and they differ depending on the treatment of posterior cruciate ligament (PS or CR TKA), the mobility of polyethylene insert (mobile or fixed bearing TKA) and the fixing method of prosthetic components (cement or cementless TKA).

Unlike the anterior cruciate ligament (ACL), which is always cut during TKA, the posterior cruciate ligament (PCL), responsible for anterior-posterior knee stability, can be preserved or not, depending on his health status. In the first case the surgeon implants a CR (Cruciate retaining) TKA, stabilized by native ligaments. In the second case a PS (Posterior stabilized) TKA: an intercondylar

plug on polyethylene insert (Post) interacts with a horizontal bar (Cam) placed on the femoral component to replicate the function of the removed ligament (Post-Cam engagement).^[5] (Fig.11)



Fig.11: CR TKA (left), and PS TKA (right).

In the fixed-bearing TKA, femur rolls on the cushion surface of the tibial insert, so one of the biggest complications is the wear of the polyethylene. To reduce this problem, in mobile-bearing TKA, the insert can rotate short distances on the polished tibial tray and its surface is more congruent to the femoral component, to spread the loads. However, this type of TKA requires more support from soft tissues so it's suitable just for young or active patients; furthermore there are no studies which shows better durability or improvement in pain and function: so, fixed bearing TKA are usually more common.^[6] (Fig.12)



Fig.12: Mobile bearing and fixed bearing TKA.

Two types of fixation are used to hold the knee implants in place: Cemented fixation uses fast-curing bone cement (polymethylmethacrylate PMMA). Cementless fixation relies on new bone growing into the surface of the implants: to encourage this process, they are made of specific materials and often they are textured or coated. [7]

1.3 Instrumented knee implants: state of the art

Total knee arthroplasty (TKA) has revolutionized the quality of life for millions of patients and has proven to be a cost-effective and reliable treatment for symptomatic osteoarthritis of the knee. An estimated 700,000 TKAs are performed in the USA each year, making it one of the most common procedures annually performed with a projected increase in demand to over 3.48 million procedures (601% of implantation rate) by 2030. [8,9,10]

Furthermore, TKA surgery is expanding to younger and more active patients [10]: because of their higher level of activities and functional demands, longer remaining life expectancy, and the greater prevalence of obesity [11] there is need to improve stability and longevity of the implants and to make them more performing.

In general, the TKA is not a permanent solution: its 10-year survival rate is considered 90%–98% and some studies even reported the 15 to 20-year survival rate is as high as 96%. [12]

After the failure of an implant, resulting in difficulties or pain during motion, the surgical procedure is repeated to replace damaged components: this revision TKA is often complex, expensive and invasive, so it's best to avoid it.

The most common causes of failure after TKA are polyethylene wear (45%), infection (26%) and aseptic loosening (17%); additional causes are instability, extensor mechanism problems, aseptic necrosis of the patella, periprosthetic fracture, and arthrofibrosis. [12]

Considering the prosthesis together with the soft tissue envelope that surrounds the knee, any surgical error or excessive deviation from the standard knee anatomy will affect TKA performances: misplacement or wrong sizing, affecting loads on the interfaces and tensions in ligaments, lead to non physiological knee biomechanics. [13]

But sometimes, surgeons are not able to understand and explain the negative performances of the TKA, because the patient's medical images "looks good" but the patient is not satisfied: about 1 in 5 patients undergoing TKA are dissatisfied with the results of their surgery. [14]

For all these reasons, despite its enormous success, the TKA is still undergoing improvement.

In order to solve the limitations of the TKA and to satisfy the patient's needs, manufacturers need to deepen their knowledge of knee Biomechanics as much as possible: this is the starting point for improving the design of existing prostheses and creating new ones.

For this purpose, numerical modeling is one of the most used methods, alone or in combination with experimental testing: the models can simulate various configurations of the knee and analyse its biomechanics for in a non-invasive, quick and cheap way.

In the rigid body analysis, the articulated bodies (bones) form a tree-like system: their motion is influenced by external forces (applied by the muscles, gravity, and the environment) and the constraints imposed by the joints. Current methods for estimating muscle, articular contact and ligament forces in the knee have evolved from first methods published in the 1970's ^[16,17], with the aim to solve the muscle redundancy problem (more unknown muscle forces than equations available from rigid multibody dynamics). Furthermore, another issue is their strong dependence on external inputs: kinematic data, external forces (ground reaction forces) and muscle activation (EMG) are needed to correct the problem of inverse dynamic and they are often invasive or inaccurate.

In particular, kinematics data are achieved by different methods including in vitro cadaveric measurements, gait analysis with motion systems, roentgen stereophotogrammetric analyses, quasidynamic MRI testing, and in vivo video fluoroscopy. Studies on cadaveric knees suffer from the difficult estimation and setting of the loading conditions in vivo and from the inability of actuators to reproduce loading and motion conditions accurately. Roentgen stereophotogrammetric analyses often have been performed under nonweightbearing conditions but are quasidynamic. In the instrumented gait analysis, owing to motion of the skin markers relative to the underlying bone, critical motion artifact may occur ^[17]. In vivo videofluoroscopy enables the reconstruction of three-dimensional (3D) position and orientation (pose) of the knee prosthesis components more accurately unhindered by the soft tissues around the joint.

Registration algorithms estimate the pose of the components from single-plane projection views on fluoroscopic image series. This method has the advantage of testing under in vivo, weightbearing, fully dynamic conditions, while subjects perform various motor tasks. In addition to standard joint kinematics, fluoroscopybased 3D techniques have largely been used but often they are non accurate.

However, combinink kinematics data with a mathematical model, substantial variations in

calculated forces exist. Morrison calculated joint forces of 2-4 BW (body weight) during level walking ^[15]. More recently, using a similar computational approach, most studies report the same range of values ^[19,20,21], other studies calculated contact forces of 5 BW (Mikosk, 1988) and even up to 6.7 BW ^[22,23]

Finite Element Modeling (FEM) is the most recent numerical technique: such analytical method allows researchers to change certain parameters of potential influence (e.g. Different designs or sizes or malalignment^[24]) and investigate their effect under standardized conditions simulating knee function in a non-destructive and repeatable manner.^[25,26] Lastly, a novel technique utilizes real in vivo 3D kinematics obtained from fluoroscopy as input for FE models of the prosthesis.^[18] Nevertheless, modeling is a challenging topic because to obtain accurate models that allows relevant conclusions, they have to be validated: experimental measurement of knee biomechanics provides a valuable opportunity for models validation.

To overcome uncertainties of numerical models or to validate them, the forces acting on the human skeletal structure can be measured with pressure sensing devices. Among such devices, the Tekscan system (I-Scan TM, Inc., South Boston, MA), is the most common used in biomechanical applications. Force is measured in real time at each sensel of the sensor, that is electrically isolated, contact areas can be measured and thus pressure profiles can be represented on the computer screen during loading in real time. The Tekscan system offers several types of sensors for pressure measurement, depending on the dimensions of sensing areas. It is commonly used for the tibio-femoral joint analysis, to study the polyethylene wear in the tibio-femoral insert ^[27] or to validate FEM models ^[26,28], and it is a particularly useful tool for the analysis of patellofemoral joint and post-cam engagement, why difficult to study analytically and still poorly understood.

The experimental tests on different types of implants show that the PF force is incredibly high, up to 7.5 BW during squat, and mostly affected by patella height (increases in patella-alta configuration^[29]) and by anterior tibial component (decreases at a mean of 2.2% for every millimetre of posterior translation of the tibial component ^[30]).

As regard the post-cam engagement, the experimental tests on different designs show high contact force (1.4 BW) and stress ^[31] and a positive correlation was found between contact force and initial contact angle. ^[32]

Even with its good characteristics as the wide range of loads measurement, the capability of produce realtime data and the great accuracy, the Tekscan system has been shown to have some inherent variability when comparisons are made across different measurement systems. The

measured errors for the Tekscan system ranges from -2% to 3% for average pressure and contact areas ^[33]. Furthermore, this sensor is quite bulky, fragile and expensive.

Another alternative for the measurement of forces acting on the human skeleton in vivo, is by means of instrumented orthopaedic implants.

This approach has been used first for instrumented hip prostheses. Strain gauges attached to implants or directly to bone and connected by transcutaneous wires to outside measuring systems have been used, but this solution is suitable only for short-term postoperative recordings ^[34,35,36].

The first implantable telemetrized device for TKA analysis was an instrumented massive distal femoral replacement for patient suffering from cancer. A mathematical approach was still necessary to get the loading data at the knee joint line level and the estimated forces in the knee joint (2.2, 2.5 BW) during level walking were smaller than those calculated anatically.^[37]

To measure the tibio-femoral contact force directly, instrumented knee implants were also developed, to perform experimental tests in vivo and in vitro (on cadaveric specimens or on Knee robotic simulators).

An initial design developed by Kaufman in 1996 ^[38] and tested in vitro in cadaveric studies ^[39], measured the total axial force and calculated the center of pressure as the point about which all applied forces had zero moment. The customized transducer consisted of a standard tibial component to which were applied four uniaxial load cells instrumented with strain gauges in a full Wheatstone bridge: the output signals from the transducers were connected directly to the data acquisition system.

This prototype was improved by D'Lima et al. inserting a radiofrequency transmission of data, and and it was tested in vitro ^[40] and intraoperatively ^[41]. In addition, the system also worked during in vivo tests ^[42]: tibial force data were recorded simultaneously with motion capture data and vertical ground reaction forces from force plates during walking, chair sit to stand and stand to sit, stair ascending and descending, squatting from a standing position, and golf swings. Furthermore, there was a first effort to calculate the percentage of axial force in the medial and in the lateral side using kinematics and force data. For all activities, total compressive load exceeded 2 times body weight, and for most activities 2.5 times body weight (approximately 3.5 BW during stair ascending and descending). Most activities placed a greater load on the medial compartment than the lateral one.

^[43]

A second design developed by the same group enabled the measurement of all six force and moment components ^[44]. Based on a commercially available prosthesis, this instrumented tibial

tray was an assembly of two structural components: the proximal section, holding the polyethylene, was connected to the distal component cemented to the tibia. The proximal section was the sensing element instrumented with strain gauges, signals of which were transmitted by telemetry. (Fig.13)

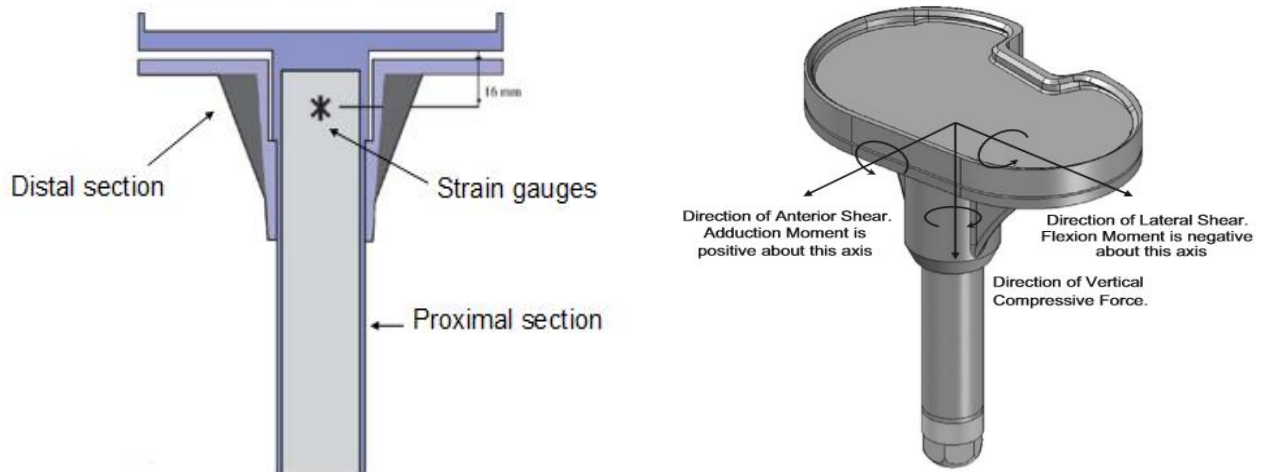


Fig.13: Multi-axis instrumented prosthesis by D'Lima et al. [44]

In 2008 the same research group made the first simultaneous in vivo measurement of six-DOF tibiofemoral forces (with the instrumented implant) and 3D articular contact kinematics (with a dual fluoroscopic imaging system) in TKA patients. The combination of these two data was used to determine the percentage of tibio-femoral loads in the medial and lateral side.

During walking, total axial forces between 1.8 and 2.8 BW were measured and in general the loads were higher in the medial compartment. During all investigated activities, the shear forces were substantially lower than the axial forces. Peak anterior shear forces of 0,3 BW were observed during walking. [45,46]

This prosthesis is currently used for the annual “Grand Challenge Competition to Predict In Vivo Knee Loads” based on a series of comprehensive publicly available in vivo data sets for evaluating musculoskeletal model predictions of contact and muscle forces in the knee. The data sets includes tibial contact-force from this instrumented tibial prosthesis, video motion, ground reaction force, muscle EMG, muscle strength, static and dynamic imaging, and implant geometry data.

Competition participants create musculoskeletal models to predict tibial contact forces without

having access to the corresponding in vivo measurements. [47]

Another group, led by Bergmann, has developed in 2007 an instrumented telemetric tibial tray, also in this case composed by two concentric hollow tibial stems (Fig.14). The proximal plate carried the snaplock mechanism for the tibial polyethylene insert, whereas the distal plate is cemented onto the resected tibia. All electronics and strain gages are housed in the cavity of the inner stem, are powered inductively and transmit the six load components telemetrically at radio frequency with a measuring error below 2%. [48]

This instrumented tibial tray was tested in vivo to measure the tibio-femoral contact forces and moments [49,50]. During the measurements, the patient's activities are video-taped and recorded together with the loads. Additionally, gait data was also captured to split mathematically the medial and the lateral contribution of the tibiofemoral force, in post-processing. Synchronous load and video data from many activities can be accessed from the free public database www.Orthoload.com [49]. The loads were measured in the Julius Wolff Institute of the Charité in Berlin directly in patients by using this instrumented implant. OrthoLoad supplies numerical load data and videos, which contain load-time diagrams and synchronous images of the subject's activities.

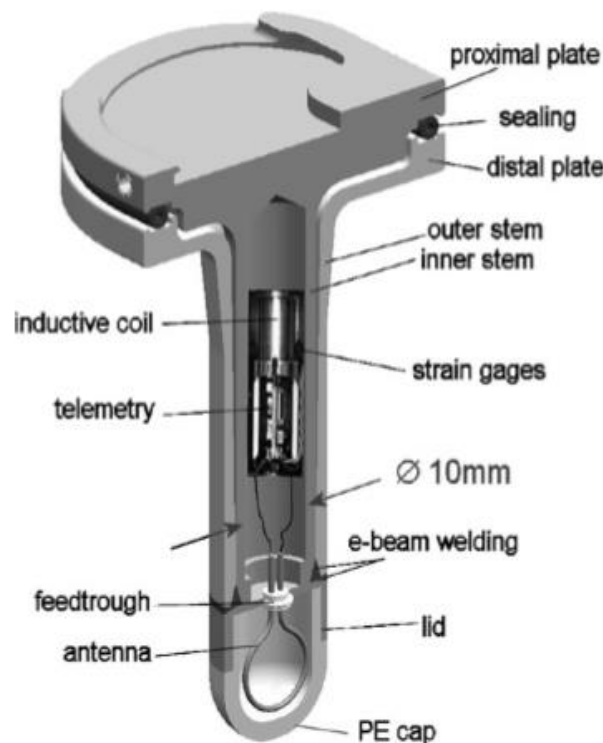


Fig.14: Multi-axis instrumented prosthesis by Bergmann et al. [48]

In order to provide a smart prosthesis design which does not impose major modification in the mechanical design of the commercially-available prostheses and gives not only in-vivo force information but also accurate kinematics, in a recent study of Arami et al. all the electronics were housed in the polyethylene insert (PE) of the prosthesis.

For measuring the kinematics of the prosthetic knee, a magnetic measurement system was designed, consisting of a permanent magnet attached to the femoral part (FP) and three 3D anisotropic magneto resistance (AMR) sensors inserted in the PE. Furthermore, strain gauges were positioned inside the PE to measure the total force applied to the prosthesis and the medial-lateral imbalance.

The proposed instrumentation is a promising system for monitoring medical implants, but overall during the surgical operation to help the surgeon in the balancing phase, because his range of measurement is quite low. ^[51]

2. Aim of the thesis

All previous studies reveal a certain disparity between the knee forces typically estimated by numerical models and those experimentally measured with instrumented implants. Moreover, the instrumented prosthesis developed until now presents several limitations: the medial and lateral tibiofemoral force distribution is achieved combining force data and kinematics data, registered through inaccurate (such as gait analysis and motion capture ^[49,50]), or invasive (like dual fluoroscopy imaging system ^[45,46]) procedures. In addition, no study has been reported about an instrumented implant that considers also the patello-femoral joint and the post-cam engagement. Moreover, within an experimental set-up with knee robotic Simulator, these prototypes are not adequate to carry out comparative tests between different designs, as modeled on specific prosthesis types.

Another issue of experimental techniques for the study of TKA, is related to the use of Tekscan system: despite being an effective tool it is very expensive, fragile, unwieldy and it has a low resolution.

For all these reasons, the experimental study of kinetics and kinematics of TKA in a research laboratory is particularly difficult and there is a need for an effective, innovative and inexpensive tool that overcomes the limitations of existing measuring instruments.

The aim of the thesis was to design and realize an instrumented total knee prosthesis to be implanted on a knee robotic simulator, for studying kinetics and kinematics of different interchangeable designs of prostheses during various activities. This thesis is just the first step of a five years research project of BEAMS Department in ULB (Université Libre de Bruxelles) which, in later stages, will also be tested on the knee robotic Simulator of the Biomechanics Laboratory. So, the tool was designed focusing only on research application, not aimed for an industrial implementation or in vivo implantation, therefore biocompatibility of materials and encumbrance were not required as a specification. Rather, the specifications were that the device was cheap, easy to manufacture within the mechanical laboratory of the Department, and easy to mount on a robotic knee simulator.

Furthermore, the project started with the aim to overcome the limitations encountered in the two prototypes of instrumented implants documented up to now.

It was supposed to be customizable, that is able to test different designs of prostheses without

altering its kinematics, it was supposed to differentiate the contribution of medial and lateral tibio-femoral forces accurately and non-invasively, and it was supposed to consider also the patello-femoral joint, always neglected in the previous works.

The information furnished by this kind of device are rather could be helpful for clinicians, engineers and researchers.

In fact it can be used to validate existing numerical models of the knee and of TKA that are currently used to estimate knee forces and kinematics, and to develop more accurate models. Furthermore it can lead to refinement of surgical techniques and to enhancement of prosthetic design that will improve the function, quality of life, and longevity of total knee arthroplasty. In conjunction with measured knee kinematics, accurate knee force data may also be used to design more effective in vitro knee testing rigs and knee wear simulators that can accurately model knee function and prosthetic wear.

Once validated, and if properly modified, an additional use of this device could be intraoperative measurement of forces to determine soft tissue balancing, evaluation of the effects of rehabilitation, external bracing, and activities more vigorous than those of daily living (such as athletic and recreational activities).

Given the current increase in the number of older persons who are at higher risk for chronic musculoskeletal disorders, and therefore of knee prosthesis, a significant positive impact on clinical outcomes and patient health care could be also anticipated as possible benefit of this research project.

3. Materials and methods

As previously mentioned, the purpose of the thesis is to develop a device for simultaneous measurement of kinetics and kinematics of several interchangeable TKA designs, to be mounted on a robotic knee simulator in the context of experimental set-up.

In particular, thanks to this device it will be possible to detect the movements and the internal forces acting in two regions of interest:

- Tibio-femoral joint
- Patello-femoral joint

To realize the project, the starting point was a knee prosthesis available on the market and being studied at BEAMS Department: Gemini SL fixed bearing PS implant (Link - Hamburg, Germany) for total knee replacement was used as model for the study of tibio-femoral joint. In addition, Genesis II Total Knee System (Smith&Nephew – London, United Kingdom) patella surface replacement was considered for the study of patello-femoral joint (Fig.15). This choice is for having the most complete composition that a knee replacement may have, in fact there are all possible articulations between prosthetic components to be evaluated: tibio-femoral joint, patello-femoral joint, post-cam engagement.



Fig.15: The original prostheses used as models. On the left, the total knee replacement (Link), on the right the patella resurfacing (Smith & Nephew).

The original geometrical shape of the prosthesis has been modified to accommodate specific sensors and simplified to be easily realized in a mechanical laboratory: the final version of the instrumented knee prosthesis is a compromise between simplicity and functionality.

In addition, the prosthesis has been transformed in a customizable device able to test different types of prostheses without modifying their kinematic and kinetic behaviour and within a limited budget.

The work has been realized in three phases:

- Analytical study
- Design
- Manufacturing

3.1 Analytical study

To understand a complex system such as the articulation between knee prosthesis components, it is useful to schematise the structure through a simplified model: this step makes the force analysis much easier and immediate.

In particular, the preliminary study of the model allows to understand what exactly are the forces between the articulating surfaces and how they are distributed in the regions of interest.

These informations are useful to answer three questions about the sensors to be used:

What types?

How many?

Where to put them?

In the simplified 3D model of the knee prosthesis, each articulating component is represented with a regular geometric shape to reduce the complexity of the problem and better identify the contact areas of the joints.

Furthermore, several assumptions are made in the model:

- the sliding components are assumed to be rigid bodies: consequently, disregarding the deformation of materials, the contact areas reduce to single points in which contact

pressures are concentrated and represented by three-dimensional force vectors;

- the materials of the prosthetic components are considered to have a linear elastic behaviour: so, the superposition of effects is applicable;
- the movements of the prosthesis are assumed to be infinitely slow (quasi-static analysis) so at each instant the equilibrium equations of the rigid bodies are applicable:

$$\begin{cases} \sum \vec{F} = 0 \\ \sum \vec{M} = 0 \end{cases}$$

Where:

$\sum F$ = Sum of all Forces acting on the rigid body;

$\sum M$ = Sum of all Moments acting on the rigid body.

In a model with 3 degree of freedoms (DOFs), it is a system of six scalar equations.

Before starting the analysis it is appropriate to define the 3D reference system of the model compared to the anatomical one: (Fig.16)

z axis = longitudinal axis (axial direction of motion)

y axis = sagittal axis (antero-posterior direction)

x axis = transverse axis (medio-lateral direction)

zx plane = frontal plane

zy plane = sagittal plane

xy plane = transversal plane

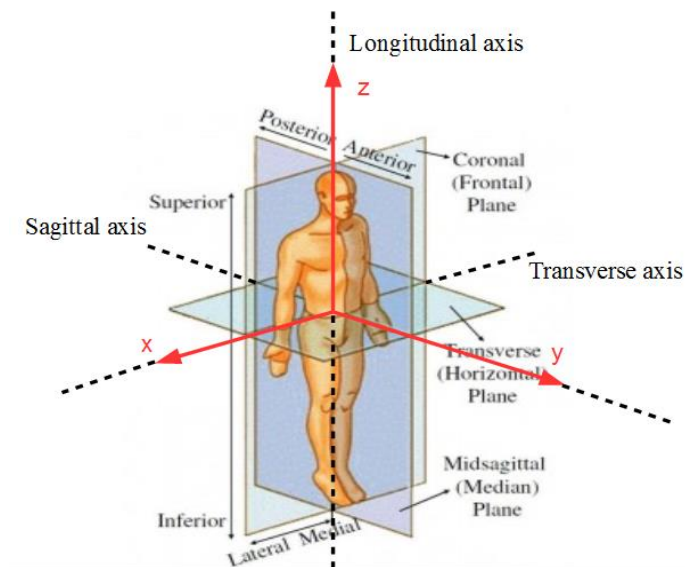


Fig.16: Reference system of the model compared to the anatomical one.

The analysis of the model was carried out separately for the two regions of interest:

- Tibio-femoral joint;
- Patello-femoral joint.

3.1.1 Tibio-femoral joint

This joint is formed by the articulation of the femoral component on the tibial insert.

In particular, considering the tibial insert, there are three contact areas in which analyze the interaction forces with the femoral component:

- medial and lateral compartment of the tibial plateau, on which act the corresponding femoral condyles separately;
- the posterior surface of the post, on which acts the cam of femoral component, forming the post-cam engagement.

Before starting the analysis, it is appropriate to make several considerations:

1. The femoral cam pushes on the posterior surface of the post mainly perpendicularly: so, the post-cam force is considered as a unidimensional vector along the AP direction (y axis), and it appears only in the bidimensional model on the sagittal plane.

In the sagittal model (Fig.17), the femoral condyles are represented by best-fit circles, the cam is represented by a cylinder, the posterior side of the post is represented by a vertical plane and the tibial plateau by an horizontal plane. In addition, the cam works on the posterior surface of the femoral post that has both a reduced area and thickness: therefore the available space to accommodate sensors is greatly reduced.

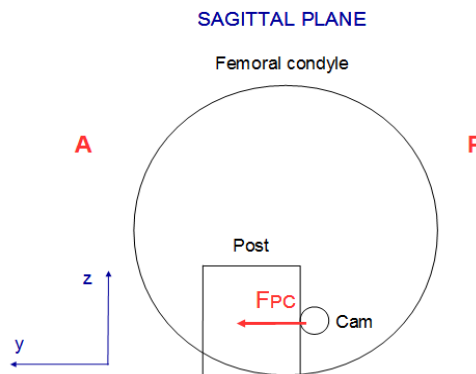


Fig. 17: Bidimensional sagittal model of post-cam engagement.

For these reasons, considering the good results obtained in previous experimental tests on post-cam engagement ^[31,32], the kinetics and kinematics of this joint can be measured with the uniaxial Tekscan pressure sensor. This solution works without changing the original structure of tibial insert (and therefore without distorting original kinematics of the prosthesis) and without neglecting significant force components. In the analysis of the tibial insert model the post-cam force is ignored, as its behaviour is measured independently: its contribution can be added separately at the end of the analysis.

2. The behaviour of the tibio-femoral joint is not symmetric, so the informations in the medial compartment are needed separated from the lateral one, but the transmission of forces from one side to the other prevents to make a differentiated analysis. Having ruled out the possibility of dividing into two parts the insert to avoid the crosslink (the cut would affect too much the kinematics of the prosthesis), the tibial plateau is assumed as a single piece, on which at the same time act two unknown forces, the medial and the lateral tibio-femoral forces.
3. In this first phase of the work the purpose is just to choose the sensors: so, to simplify the calculations, only the axial components of tibio-femoral forces are considered. In the design phase, the sensors will be positioned so that the user can choose to calculate also the remaining components, if he wanted to.

The analysis of the model took place in all three anatomical planes but to avoid repetitions and redundancies only the frontal view is represented because it is more representative.

In the simplified frontal model of the tibial insert the femoral condyles are represented by circles, the tibial plateaus by flat horizontal planes.

The Fig.18 shows the bidimensional model of the tibial insert: the most interesting aspects to be studied are the kinematics of the femoral component the asymmetric distribution of total axial force between medial and lateral sections, the varus/valgus moment along y axis.

For this reason the unknown variables to be calculated are:

- coordinates of contact points between the condyles and the tibial plateaus (a and b);
- tibiofemoral total axial force and its medial and lateral components (F_m and F_l);
- varus-valgus bending moment (M_{vv}), due to the asymmetry of the tibio-femoral forces.

The idea of using a single sensor to obtain both kinetics and kinematics informations (as for the post-cam engagement) was quickly discarded. In fact the pressure sensors currently available on the market (like the Tekscan) dynamically measure the contact zones, areas and pressures, but ignore the shear force components and the moments. For this reason, the idea of using two different types of sensors was evaluated.

By placing a multi-axial load cell (that is able to measure three-dimensional forces and moments) below the tibial insert, at the origin of reference system, its measured compression axial force value (F_{s_z}) and bending moment along y axis (M_{s_y}) can be inserted in the frontal model.

Applying the static equilibrium of forces and moments in the frontal plane the the diagram is described by the following equation system*:

$$\begin{aligned} \sum F_z = 0 &= F_{s_z} - F_m - F_l \\ \sum M_y = 0 &= M_{s_y} - F_m \cdot a + F_l \cdot b \end{aligned}$$

The multiaxial load sensor alone is not enough to fix the system, which has two equations and four unknown variables (F_m , F_l , a , b): to split the total axial force in the medial and lateral contributions there is need to reduce the number of unknowns variables from four to two. Using the kinematic data, and then knowing the y-coordinates a and b , the system becomes solvable.

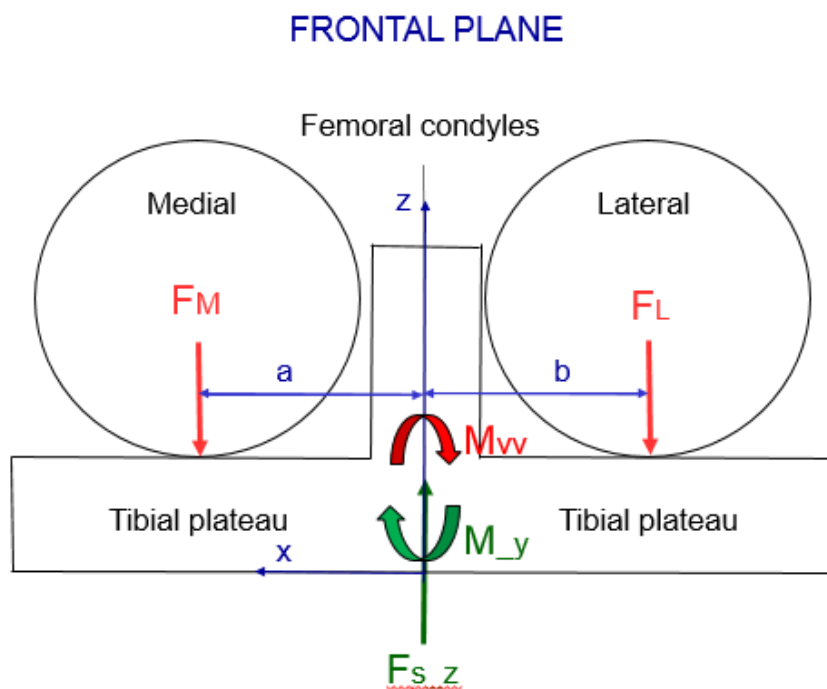


Fig.18: Bidimensional frontal model of tibial insert, including the force sensor.

Then, as well as in the instrumented implants made so far ^[44, 48], the subdivision of the total axial force in the medial and lateral contributions has to be made mathematically, combining the kinetic data with cinematic ones to solve the equilibrium system.

As regard the remaining two anatomical planes (transverse and sagittal planes) and the corresponding two-dimensional views of the model, the analysis and its results are the same. There is need for both a position sensor and a mult-axial load cell: in the transverse plane the load cell has to measure the flexion-extension bending moment and in the sagittal plane the intra-extra rotation torsional moment.

In conclusion, the theoretical analysis of the tibio-femoral joint reveals that, in order to know its kinetics and kinematics, the tibial insert must be instrumented through three sensors: the Tekscan sensor on the posterior surface of post plug to study the post-cam engagement, a position sensor on the tibial plateaus, and a multi-axial load cell in the bottom surface in contact with tibial tray. Combining and synchronizing the sensor outputs it is possible to have an overall idea of the tibiofemoral joint Biomechanics: the femoral condyles kinematics, the forces that it exerts on tibial insert and how they are distributed between the medial and lateral compartments, bending and torsional moments of tibio-femoral joint.

3.1.2 Patello-femoral joint

The patello-femoral joint is composed by patellar insert of the prosthesis articulating with the femoral component trochlear groove. The experimental results found in the literature and obtained by means of Tekscan highlight a characteristic behavior of patello-femoral joint: during a complete cycle of knee flexion/extension, the contact between the two components of the joint occurs at a single point, in two points, or doesn't happen at all, depending on the angle of flexion and the patellar shape. This requires instrumenting the patellar insert so that it is able to cope with all these cases.

The simplified model of the patello-femoral joint in the sagittal plane is shown in Fig.19.

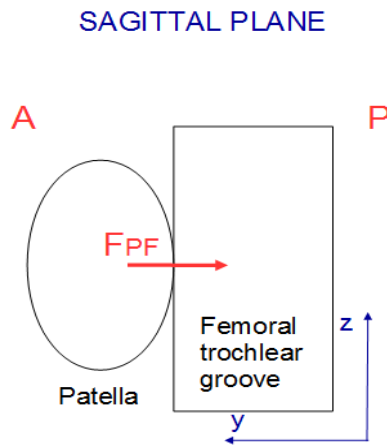


Fig.19: Bidimensional sagittal plane of patello-femoral joint.

The patellar insert has a regular elliptical shape and the internal force of the joint is represented by vector F_{pf} .

Following the same procedure of tibiofemoral joint, and solving the static balance of the rigid bodies in the bi-dimensional anatomical planes, the conclusion is the same: even in this joint, to have complete data on kinematics and internal loads, the best solution is to install two different types of sensors. A multi-axial load cell has to be installed at the back of the patellar insert to measure forces and moments values, a displacement sensor has to be placed on its surface to investigate the contact points with the femoral groove.

Kinematics data obtained from position sensors are particularly interesting when the contact points are doubled and can also be combined with data from the load cell to split the contributions of forces just like it does in the tibial insert.

3.2 Design

The theoretical analysis of simplified model revealed the need for instrumenting the prosthesis with two kinds of different sensors: one multi-axial load cell and one position sensor. The installation of the force sensors below the polyethylene inserts implicates several adjustments in the original prosthetic structure, while the position sensor must be installed on the surface of the tibial and patellar inserts, not affecting the original geometry of the prosthesis. So, as the two sensors are totally independent of each other, they were designed separately and in parallel.

3.2.1 Force sensing

First a thorough research on the market was made, to find a commercially available load cell with the right specifications, in order to fix it by bolts between the tibial tray and the polyethylene insert.

The load cell would have meet a compromise between a large measuring range, a small size and a low price: these requirements made market research particularly difficult.

■ **GEMINI® SL® Tibial Components – PS**
to used with PS (Posterior Stabilized)

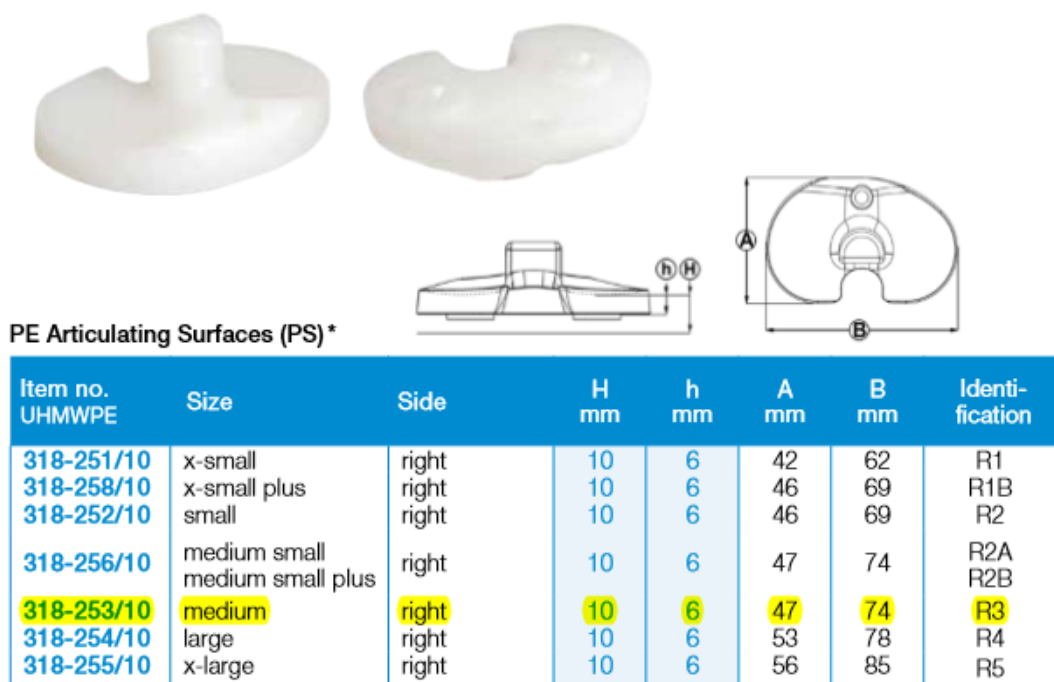


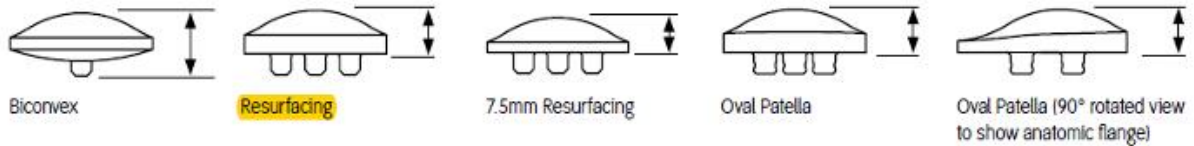
Fig.20: Datasheet of Link Gemini SL total knee replacement.

The datasheet (Fig. 20) of the prosthesis Link Gemini SL Total knee replacement chosen as model, considering the medium-size version of the right leg, shows that the tibia tray perimeter has a maximum sizes of 74 mm and 41 mm.

The patellar insert from Smith&Nephew has a diameter of 35 mm. (Fig.21)

GENESIS II Knee System

Patellar Dimensions



	Thickness (mm)	Diameter			
Biconvex	13	23	26	29	32
Resurfacing	9*		26	29	32
Resurfacing 7.5mm**	7.5		26	29	32

Fig.21: Datasheet of Genesis II patellar resurfacing, Smith & Nephew.

To promote convergence of loads on the sensing element, the load cell should have boundary sides that do not exceed the tibial tray perimeter. Moreover, it should not be too heavy and too high, especially for the patello-femoral application, otherwise the device would be too cumbersome and difficult to install within a robotic knee Simulator.

So, a maximum height of 20mm and a maximum side of 35mm were set as search parameters.

The load range needed was the other issue: the total load expected in the tibio-femoral joint is around 3-4 BW ^[20, 47, 50], therefore, considering a BW of 70kg, the load sensor need to measure at least 3 kN.

In the market this load cell is very difficult to find, but after a careful research two commercial models were selected because they match the specifications needed: Klister 3-Component quartz force sensor Type 9027C and PBC Piezotronic 3-component ICP quartz force ring Model 260A01.

In the Appendix A the datasheets of these devices are shown.

However, their price didn't agree with the budget given, and ask a company to create a customized load cell would have been even more expensive. At the end, the idea to use a load cell was not followed anymore and it has been decided to build a manufactured device cheaply, using the tools and equipment of the Department.

3.2.1.1 Instrumented tibial tray

To start the design phase, a deep study has been made about the existing different types of loadcells to study their structure, to understand their operating principles, and to choose the most suitable type to be adapted to the prosthesis.

A load cell is a transducer used to create an electrical signal whose magnitude is directly proportional to the force applied on it and being measured. The most important part of a load cell is the sensing element, a load-receiving component through which the load is applied and transduced in voltage signal. The various types of load cells include hydraulic, pneumatic and strain gauge load cells and they differ according to the force transduction mechanism; for their accuracy and low costs of realization, usually the manufactured load cells are strain gauge load cells and this type is also the most common used in industry.

Taking the cue from the literature of instrumented prosthesis, it came up with the idea of turning the prosthesis itself in a strain gauged load cell, by modifying its original shape to conform to this function and to glue the transducers.

The work was accomplished through the SolidWorks 2015 CAD software, starting from the CAD file of the original prosthesis, made available by the companies for the project. (Fig.22)

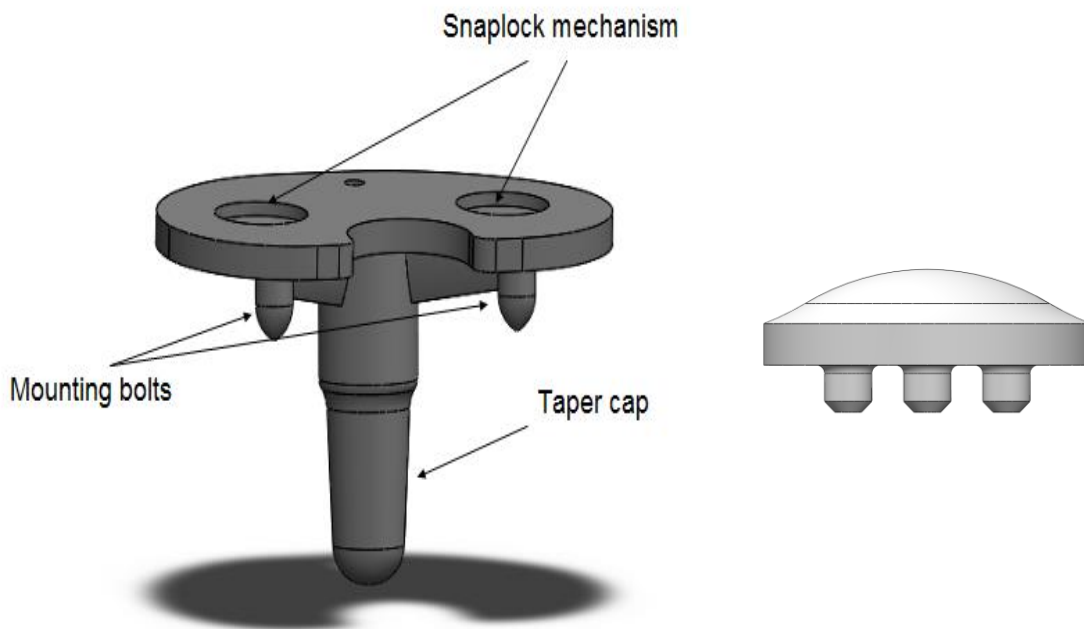


Fig.22: CAD files of the Link Gemini SL original tibial tray (left) and Smith&Neohew Genesis II patellar resurfacing (right)

As regards the tibio-femoral region of interest it was possible to take a cue from the literature because until now two different groups have built and tested in vivo instrumented knee implants for tibial-femoral forces study. Both groups used the tibial tray as sensing element because all loads and moments acting on the polyethylene insert converge on it.

Following the examples of D'Lima et al and Bergmann et al., the original tibial tray of the prosthesis was divided in two concentric parts: a proximal plate carrying the strain gauges and the snaplock mechanism for the tibial insert, and a distal plate to be fixed to the knee simulator. The strain gages were going to be housed on the surface of the inner proximal stem.

3.2.1.1.1 First design

The first design of tibial plateau has been realized by keeping the external boundaries of the original prosthesis: the mounting bolts ensured the fixing on the knee Simulator without special adaptations. Only the taper cap of the original tibial stem was removed, to permit the screwing between the concentric trays: using a filler, the design is compatible with the original prosthesis knee Simulator.

After removing the final part, the original tibia plateau has been "emptied" to permit the insertion of the sensing element of the load cell, the proximal tray (Fig.23)

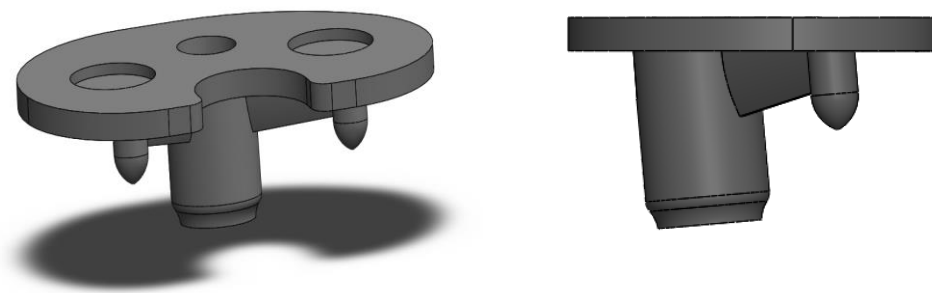


Fig.23: First CAD design of the distal tibial tray in a trimetric view (left) and lateral view (right).

The proximal tibial tray consists of a top plate and a cylindrical rod. To avoid disrupting the natural kinematics and biomechanics of the prosthesis, the top plate is perfectly compatible with the original polyethylene insert, not affecting the contact surface with femoral component, and the cylindrical rod has 5° of inclination respect to the top plate to maintain the posterior slope of the

original design. (Fig.24)

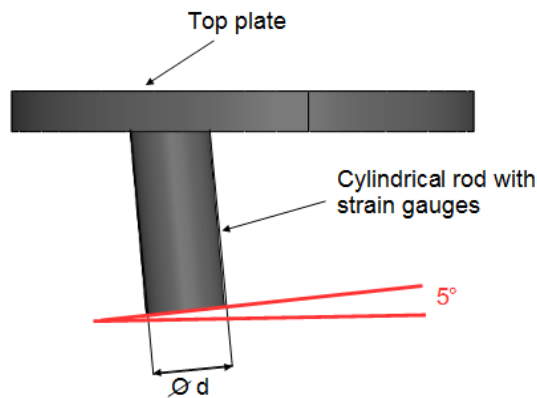


Fig.24: First CAD design of the proximal tibial tray in a lateral view. The diameter of cylindrical rod ($d=8\text{mm}$) and the 5° posterior slope are indicated.

The Fig.25 shows the assembly of the first prototype:

1. Distal tray
2. Proximal tray

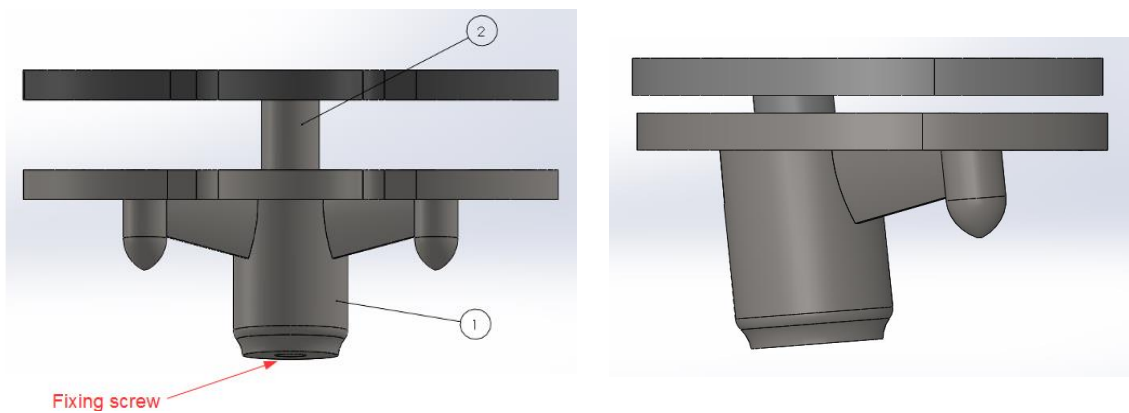


Fig.25: First CAD design of the tibial tray (assembly) in a frontal view (left) and in a lateral view (right).

The two components, joined by a fixing screw, are separated by a gap of 2 mm to allow the passage of the cables connected to the strain gauges that are going to be glued to the proximal component. For experimental testing of a prosthesis, the distal component must be cemented on the tibial component of the knee robotic simulator: by changing only the proximal tray, it is possible to test different types of prosthesis.

Despite the advantage of being fully compatible with the original knee Simulator, this design has

several problems:

- the diameter of the sensing element is too small (8mm): this increases the crosstalk between the strain gauges and makes difficult their bonding because of the reduced surface available;
- the shape is too complex to be realized in a university mechanical laboratory: the most problematic aspects are the mounting bolts, the posterior slope, and the realization of the whole piece in a single block;
- the instrumented prosthesis is not customizable: only the prostheses with a posterior slope of 5 degrees can be tested, screwing their corresponding proximal plate.
- each time a different prosthesis is tested, the cemented distal component has to be extracted to enable the screwing of its corresponding proximal plate, and this makes the device inappropriate.

3.2.1.1.2 Second design

After several ideas, according with the technician of the mechanical laboratory of BEAMS Department, these problems were solved in the second design.

The device has become modular, consisting of standard geometric elements easily workable with the equipment of the laboratory; even the measurements were made compatible with those standards.

- the proximal plate has been divided into two parts: the top plate and the cylindrical sensing element are connected by a screw. This change not only simplifies the manufacturing but also makes the device customizable: indeed, interchanging only top plate, you can test all kind of prosthesis without removing the distal tibial tray from the robotic Simulator, that can be fixed with cement.

Based on the compatibility with the polyethylene tibial insert, each prosthesis has its own top plate: in the case of the project, top plate has an inclination of 5° to simulate the posterior slope of the original prosthesis;

- the diameter (d) of the sensing element (proximal plate) has been increased up to 15 mm;
- the tibial plate of the distal tray is removed to give more space to the wiring of the strain gauges and all the fillets;

- mounting bolts have been removed, so the device becomes a support for the load cell, to be fixed to the knee simulator with a fixation cement.

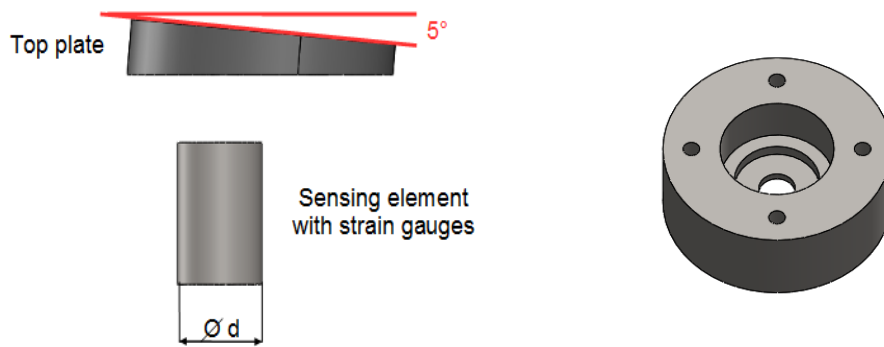


Fig.26: Second CAD design of the modular tibial tray (left) with a top plate and the sensing element. Second CAD design of distal plate(right), that becomes a distal support for the load cell.

Fig.27 shows the final design of the instrumented knee prosthesis:

1. Distal support
2. Load cell
3. Top plate
4. Tibial polyethylene insert

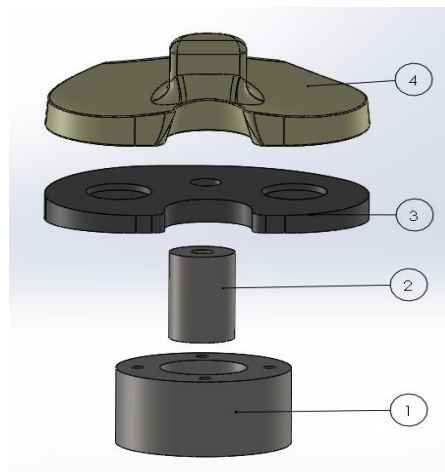


Fig.27: Second CAD design of the instrumented tibial tray with the polyethylene tibial insert.

3.2.1.2 Instrumented patella

As in the case of instrumented tibial tray design, the load cell has to be fixed taking into consideration the compatibility with the robotic knee simulator: usually the patella is fixed with a mounting block and straps, so there is need to create a structure that works as a load cell, allowing also the installation of the patellar insert on the robot.

Nevertheless, unlike the other joint, there are not examples in the literature on which to take inspiration.

Taking the cue from the second design of instrumented tibial tray has been decided to follow the same working principle: a sensing element with a cylindrical shape, through which the patellofemoral forces are transmitted, is fixed besides the patellar insert by means of an interchangeable patellar top plate.

In Fig.28 are shown the components of the instrumented patella:

1. Base support of the load cell
2. Locking mechanism containing a hole for mounting straps
3. Sensing element
4. Patellar top plate
5. Patellar insert

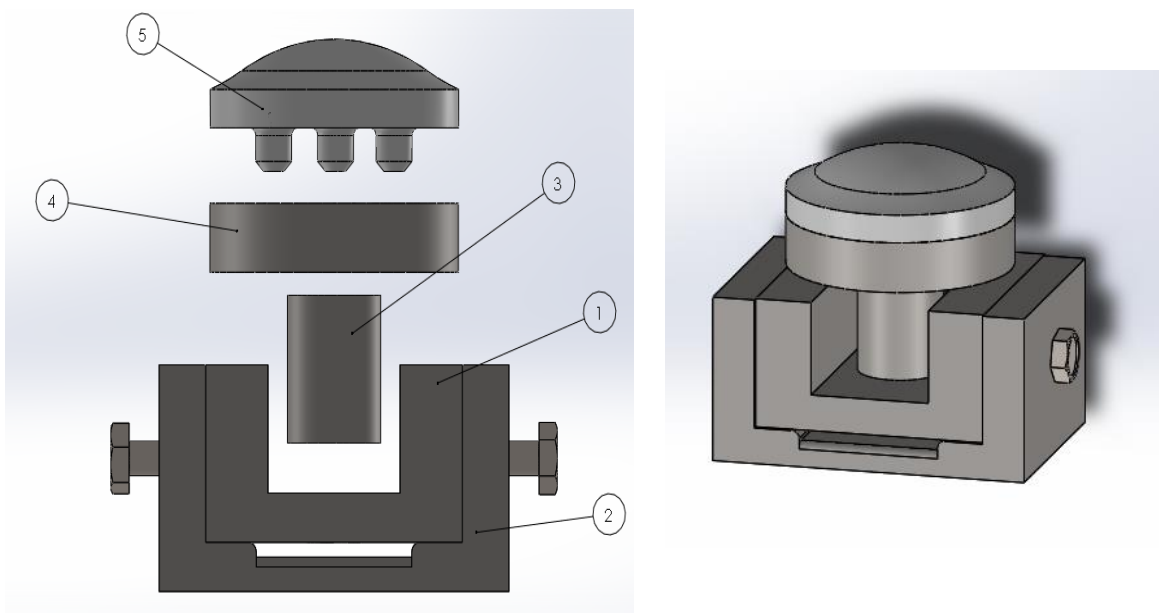


Fig. 28: CAD design of the instrumented patella with the polyethylene patellarinsert (assembly).

This modular system permits to tests different designs of ptellar inserts simply changing the top

plate, making the design customizable.

Furthermore, the sensing element is equal to the tibio-femoral one: in the case of a two-stage separate analysis for the two joints, it is possible to use the same sensing element, easily interchangeable thanks screwing mechanism.

Then, also the load cell calibration can be done only once for both joints, simplifying and speeding the testing procedure of the prostheses.

3.2.2 Position sensing

Before any other possibility, it was considered to use the Tekscan system not only as a pressure sensor for the post-cam engagement, but also as a position sensor in patellofemoral and tibiofemoral joint, because the sensor is already present and usually used in the BEAMS Department.

However, this option was quickly rejected, for the following reasons:

- It is too expensive: the aim of the thesis is to develop an inexpensive method to study the internal biomechanics of the prosthesis also in laboratories that do not have such device;
- It is too fragile: the experimental tests carried out previously in BEAMS Department revealed that, when subjected to excessive loads on surfaces that are not regular, and that is the case of the knee joints, Tekscan sensor tends to be damaged very easily. This problem can be weakened by applying a teflon tape that increases its flexibility, but the results are not satisfying;
- It's too bulky;
- It has its own software for data acquisition: this makes it difficult to synchronize and to combine the position data with force data;
- the sensel dimension is about 2x2 mm (Fig.29).

Once excluded the possibility of using the Tekscan, a long research on the market was made, to find a displacement sensor with higher performance and lower price. Inertial, inductive, magnetic, capacitive, piezoelectric, resistive displacement sensors were taken into account but no solution was found: the position sensors commercially available were too much expensive, or fragile, or

with a bad resolution. For this reason, it was decided to manufacture a position sensor in the BEAMS Department, with the following specifications: cheap, flexible, non invasive, with an improvable resolution and easily synchronizable with the forces data from load cell.

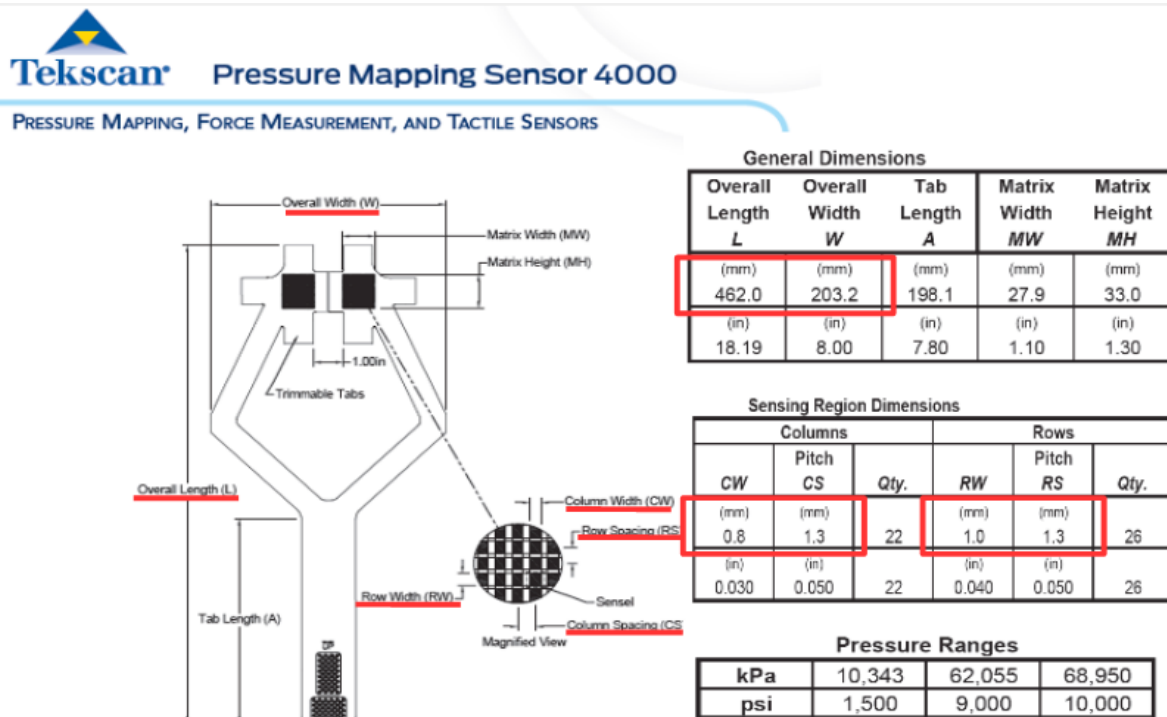


Fig. 29: Tekscan Mapping sensor datasheet.

Taking a cue from the working principle of resistive touchscreen technology, it has been decided to realize a manufactured bidimensional potentiometer.

Potentiometer is a variable voltage divider with a shaft acting as sliding control for setting the division ratio: this ratio is directly proportional to the position of the shaft, so this instrument is used as displacement sensor. In electronics, a voltage divider (also known as a potential divider) is a passive linear circuit that produces an output voltage (V_{out}) that is a fraction of its input voltage (V_{in}). Voltage division is the result of distributing the input voltage among the components of the divider. A simple example of a voltage divider is two resistors connected in series (resistive divider), with the input voltage applied across the resistor pair and the output voltage emerging from the connection between them. If one of the resistance is variable, the voltage divider works as a potentiometer: powering the circuit with an input voltage V_i , the output voltage V_x is inversely proportional to the variable resistor R_x .

The resistance of a given object depends primarily on two factors: what material it is made of, and its geometry. For a given material, the resistance is inversely proportional to its cross-sectional area

and directly proportional to its length. The resistance also depends on the resistivity, characteristic property of each material.

$$R = \rho \frac{l}{A}$$

ρ = resistivity
 l = length
 A = cross-sectional area

The piezoresistive effect is a change in the electrical resistivity of a material when mechanical strain is applied on it: as pressure increases, the resistance of the material decreases.

Then, by placing a layer of Piezoresistive material between two bodies in contact with each other, the contact point is where the resistance of the material is inferior.

The idea is to create a matrix of voltage dividers in which a Piezoresistive material sheet, inserted into the circuit, acts as a variable resistor R_x . Each element of the matrix, and then each output voltage, is marked by an x-y-coordinate: applying pressure on the matrix, the x-y- coordinate of the application point is where the measured voltage is lower. (Fig. 30)

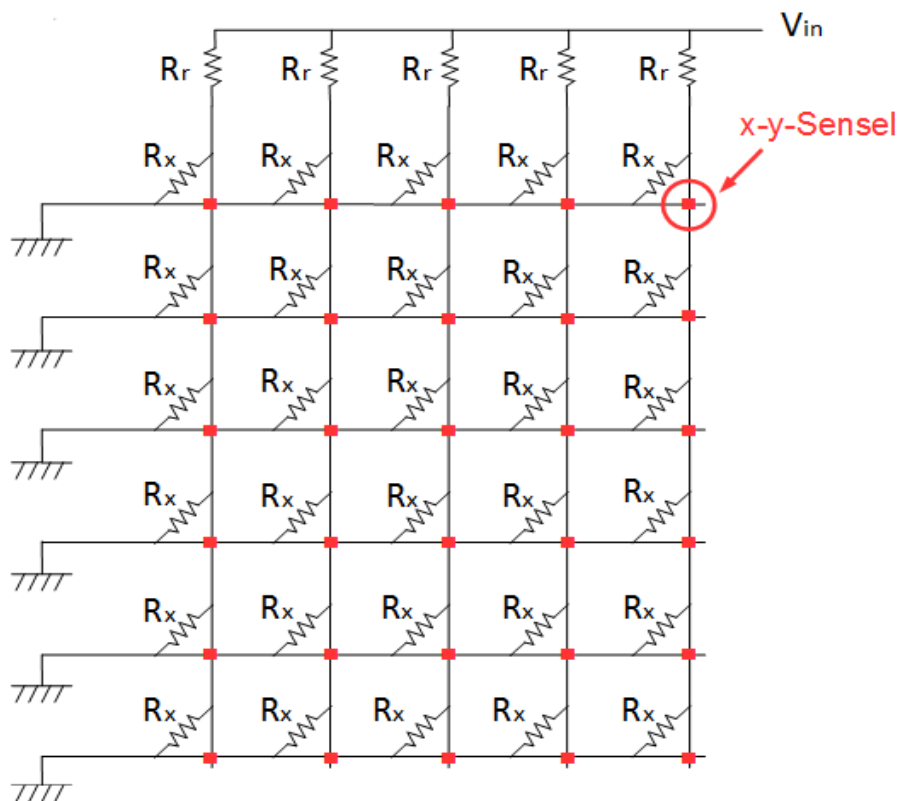


Fig.30: Matrix of voltage dividers.

In practice, this idea can be implemented using a three layers sensor: (Fig.31)

- the top layer contains vertical conductive lines, that act as the columns of the matrix;
- the second layer is a thin foil of piezoresistive material, that acts as the resistance R_x ;
- the bottom layer contains horizontal conductive lines, that act as the rows of the matrix.

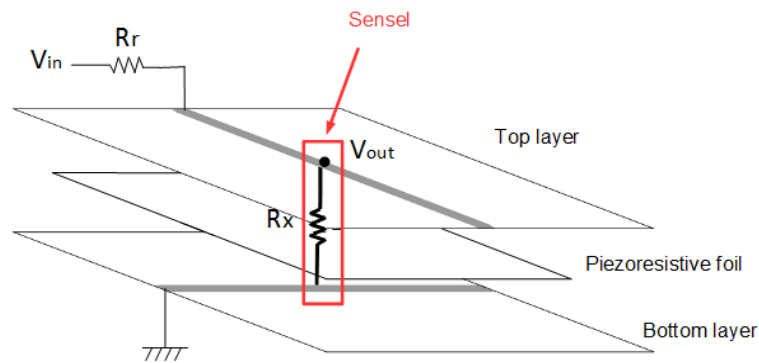


Fig.31: Three-layer sensor at a sensel point.

All the columns must be connected to supply voltage through reference resistances R_r , and all the rows must be connected to the ground through switches: when the switch is closed the row is "turned on", the electrical current can flow to the ground and it is possible to read the output voltage of each column, otherwise the row is an open circuit and it is "turned off".

To avoid short circuit of the matrix, the switches have to be controlled externally by a microcontroller, so that the rows can be "turned on" one after the other, and never together.

For each row, the output voltages of each column can be stored in an array, so at the end of the acquisition there will be a matrix of voltage values: when the sensor is pressed, the x-y-coordinate of the smallest element of the matrix is the contact point.

The three layers must be realized with flexible materials, so the sensor can be perfectly positioned on the surfaces of tibial insert and patellar insert.

Furthermore, a data acquisition system (DAQ) is necessary to power the circuit, to control the switches, to store the voltage outputs matrix and to dynamically detect the x-y coordinate of the femoral component for on the polyethylene inserts for each instant and for each movement of the prosthesis. Synchronizing and combining the position data with the force data from strain gauges the system* can be solved and the axial force can be divided between medial and lateral component.

3.3 Manufacturing

3.3.1 Six-axis load cell

The first design of the prosthesis has been modified according to both functional and practical requirements: in fact, after some meetings with the technician of the department, the design has been adapted to the manufacturing machinery and instruments of the laboratory.

Once obtained the final CAD design of the device in SolidWorks software, the 2D draftings were given to the technician of the BEAMS Department laboratory and in 3 weeks the work was completed. (The draftings are reported in the Appendix B)

The prototype has been realized in aluminium because this material is able to sustain large deformations maintaining a linear behaviour. This property is useful to increase the sensitivity of the load cell, allowing the strain gauges to detect even relatively low forces. For example, the cylindrical shape of the load cell assures a good sensitivity in measuring the bending moments, and indirectly in measuring the shear loads (see below), but the sensitivity in measuring the axial force is poor due to the high axial stiffness. Aluminum alloy partially reduces this problem because it offers a good compromise between the mechanical strength and the stiffness of the cylinder. According to the mechanical properties of aluminium (Young's modulus 71000 MPa, tensile ultimate strength 480 MPa, yield strength 410 MPa, and Poisson's ratio 0.32) and load conditions to which the prosthesis is subjected, was verified the safety of the structure.

As regard the application of strain gauges, in the ULB departments manufactured load cells are not realized and usually the strain gauges are pasted by external companies: so, not having staff whom ask for advices and not being present the suitable equipment for the pasting procedure, strain gauges have been glued in the Biomechanics Lab of Department of Industrial Engineering (DIN), University of Bologna.

Thanks to the kind collaboration of prof. Cristofolini, a three day training in Bologna was made, with the aim of acquiring all the necessary informations about the bonding procedure of strain gauges and learning about their uses in the load cells manufacturing. In three days it was possible to see manufactured load cells, how they work, to learn the strain gauges gluing procedure and to make a trial gluing.

Furthermore, after some meetings with the technicians of the department, it has been chosen

the most effective brand, types, and arrangement of strain gauges for the project, analyzing the surface available for bonding, the orientations of the forces and moments to be measured, and the construction material of the load cell: the final strain gauges types and disposition is a compromise between these specifics.

Depending on the mechanical stress to be sensed, strain gauges should be placed at the points of maximum deformation and they should be oriented to maximize sensitivity.

Considering the sensing element of the load cell in the xyz reference system of the prosthesis, there are four loading components to be measured: (Fig.32)

- One normal force along z-axis (Axial force)
- Two orthogonal bending moments along x and y axis (flexion-extension and varus-valgus)
- One torsional moment along z axis. (intra-extra rotation)

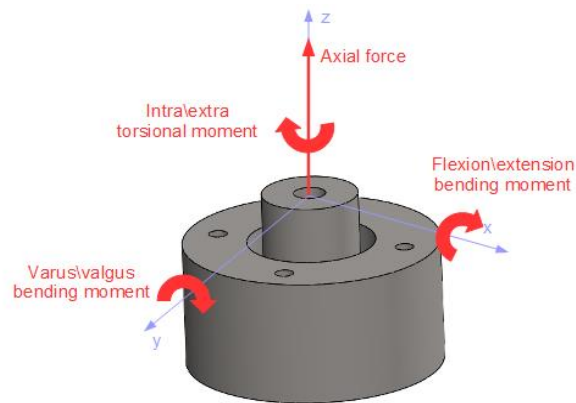


Fig.32: Load cell (sensing element and distal support) in the xyz reference system with all the unknown variables.

It was decided to use two miniaturized linear strain gauges and four miniaturized rosettes, and all the strain gauges were going to be positioned at the mid cross section of the cylinder to maximize the sensitivity for bending moments.

In Fig.33 is shown the strain gage disposition design in a superior view of the load cell: the linear strain gauges are indicated with the label L, the strain gauges of the rosettes have the label R, and they are numbered clockwise starting from the y axis, that is assumed at 0°. Four strain gauges (R1, R3, R8, R10) are connected to form a full Wheatstone Bridge for the measurement of the torsional moment M_z (Intra-extra rotation): they are oriented at 45° to maximize the sensibility to shear stress.

The two opposite strain gauges R6 and R13 are connected to form a half Wheatstone Bridge in

adjacent arms of the bridge, to measure the bending moment M_y (Varus-Valgus).

The same connection is made for the two opposite strain gauges R2 and R9, to measure the orthogonal bending moment M_x (Flexion-Extension).

The remaining four strain gauges (R4, R11, L7, L14) are connected to form a full-bridge Poisson circuit for the measurement of the axial load (this configuration enhanced the sensitivity).

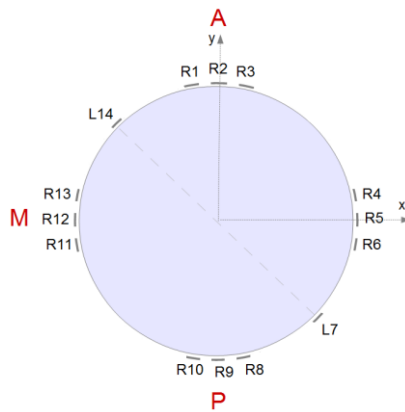


Fig.33: Strain gauges disposition in a superior view of the load cell.

The two orthogonal shear stresses can be calculated indirectly, considering them as generators of the two orthogonal bending moments, and knowing the lever arm (midcross section). The cylindrical surface of the loadcell was also developed in a planar plane: the obtained rectangle, shown in Fig.34, is useful to have a clear idea of the surface available for bonding.

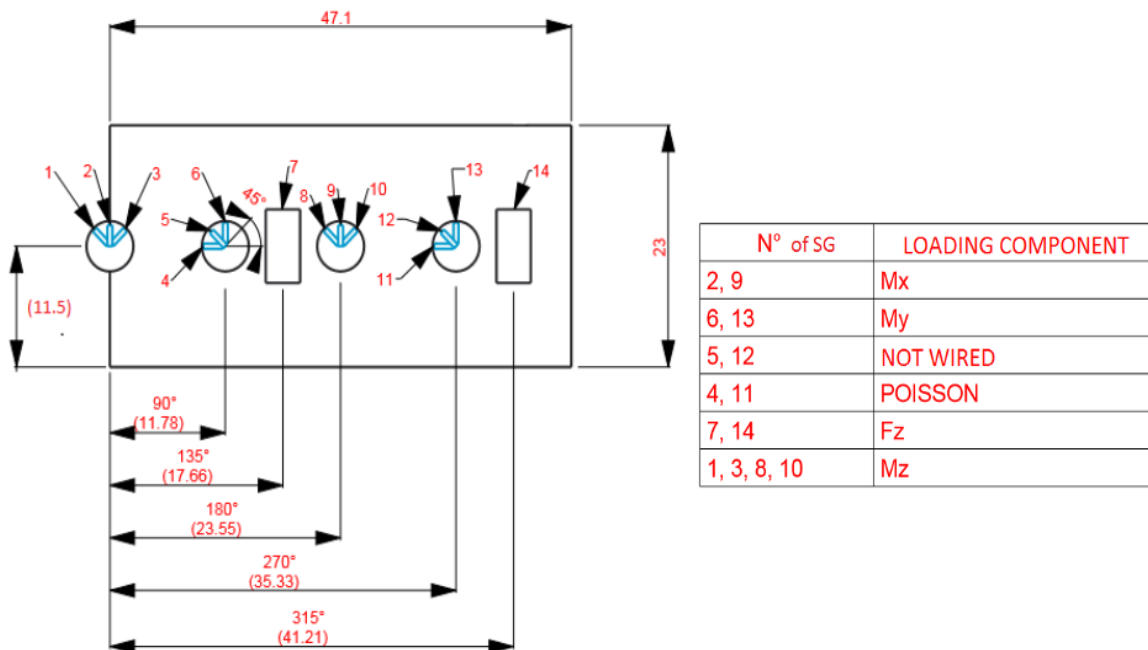


Fig.34: Strain gauges disposition in a planar development of cylindrical surface of load cell.

This step simplified the choice of the size of strain gauges, in fact the sum of their dimensions should not exceed those of the rectangle, and they must be spaced enough to avoid cross talk. At the end, miniaturized strain gauges were chosen (Tokyo sokki Kenkyujo Co., Ltd), already available in the DIN Department of University of Bologna: two foil strain gauges of UFLA – series and four 45°/90° 3-Element rosettes of UFRA - series. (Appendix C for the datasheets)

The backing of an UF-series gauge is made of polyimide-amide resin, which enables the gauge to be used in 150°C maximum. The backing is thin and it is easy to bond the gauge even on a curved surface without deterioration of the performance.

Cyanoacrylate strain gauges kit adhesive M BOND 200 (Micro Measurement - Vishay Precision Group) was selected for the bonding procedure because, as compared to bi-component glues, it is best suited for routine experimental stress analysis applications under temperate environmental conditions. This adhesive is very easy to handle, and cures almost instantly to produce an essentially creep-free, fatigue-resistant bond, with elongation capability of five percent or more. The installation procedure was entirely executed in Bologna, and once terminated the strain gauged load cell has been sent to BEAMS Department.

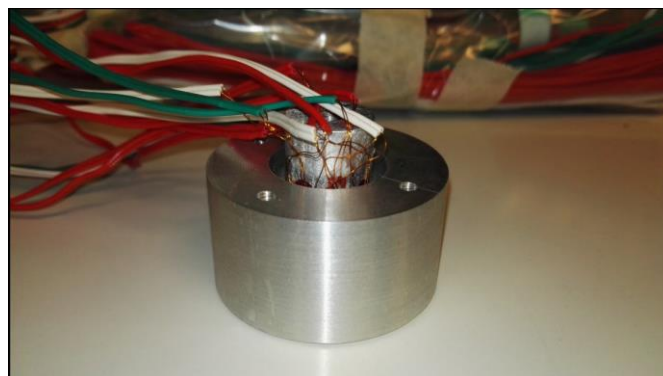


Fig.35: Strain gauged load cell sent from Bologna.

3.3.2 Three-layers piezo-resistive position sensor

The position sensor has been entirely realized in the BEAMS department, in the Micro-Bio-Mechatronics laboratory, with a laser printer for printed circuit board (PCB) Etching. Thanks to this machinery, it is possible to obtain PCB consisting of conductive tracks, pads and other features etched from copper sheets laminated onto a non-conductive substrate.

The realization of the sensor was made in four steps

1. Drawing and printing of the circuit
2. Preparation of Velostat sensels
3. Gluing
4. Soldering

STEP 1: DRAWING AND PRINTING

Both the layers of the sensor were drew using the Altium software; they contains the conductive tracks of the matrix of the circuit.

In Fig.36 it is possible to see the drawing realized in Altium , and the printed layers; both the traks for patello-femoral and tibio-femoral sensor were printed, but due to time constraints, it was decided to test only the tibio-femoral application so, from now on, the patello-femoral side will be ignored.

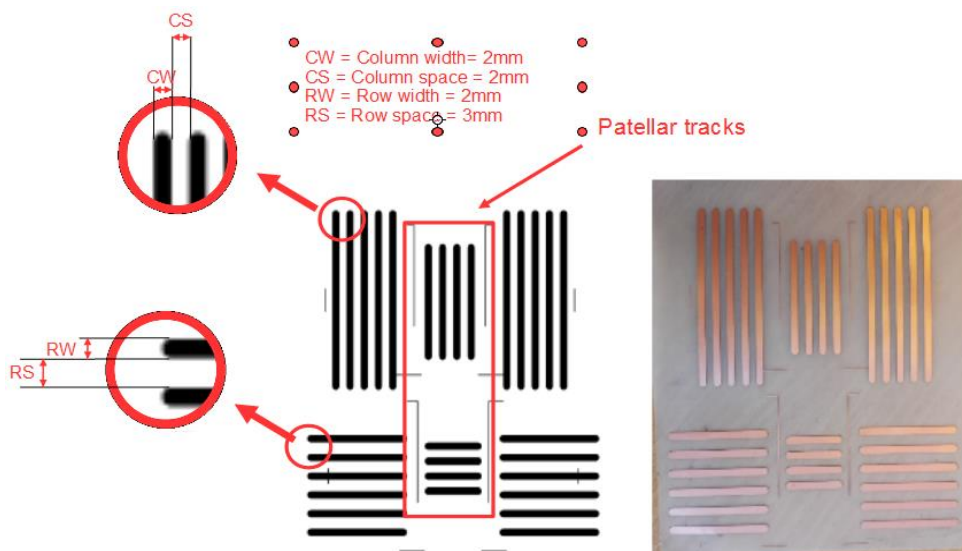


Fig.36: Drawing of the tracks (left) and printed tracks (right).

The compartments of the sensor are symmetric, so the medial side is equal to the lateral one: for both of them the first layer is composed of 5 conductive vertical lines, the second layer is composed of 6 conductive horizontal lines. The columns are distant 2 mm, the rows are distant 3 mm, and all the lines are 2mm thick: this choice was made to cover all the surface of tibial plateaus.

Overlapping the two layers, for each compartment the matrix is composed of 30 square-shaped sensitive elements, with 2 mm side.

The drawing was given to the technician of the lab, and in 30 minutes the printed circuit was already done. The non conductiv substrate of the PCB was made in a flexible material, to enable its adaptation on irregular surfaces of polyethylene inserts. Then, the PCB was cropped to get a semi-circular shape of the sensor with a tail to solder the wires; this wires-tail will be in the anterior part of the prosthesis.

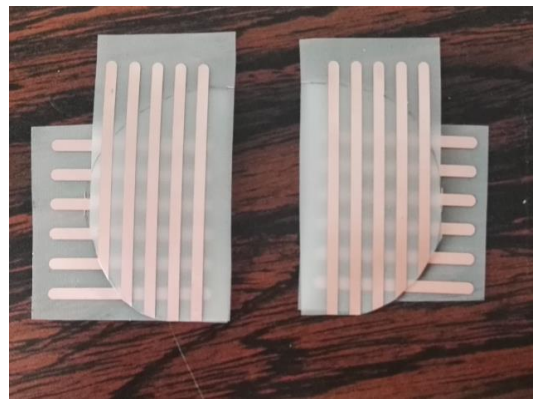


Fig.37: Cropped layers of the tibio-femoral sensors.

STEP 2: PREPARATION OF VELOSTAT SENSELS

The Velostat piezoresistive foil was used for the project: it is a polymeric foil (polyolefines) impregnated with carbon black to make it electrically conductive. It is generally used for the protection of items or devices that are susceptible to damage from electrostatic discharge and it was developed by Custom Materials, now part of 3M.

Due to its properties of changing its resistance with either flexing or pressure it is becoming popular with hobbyists for making inexpensive sensors for microcontroller experiments.

To avoid parasitic resistance between the lines, which would worsen the resolution, the Velostat layer was positioned only in correspondance of the sensor's sensels: for this reason, little squares of Velostat with 2mm side were cut out.



Fig.38 :Velostat square sensels.

STEP 3: GLUING

To keep the layers of sensor linked together and prevent Velostat squares moved from their positions, causing a short circuit, some glue was applied between the layers. CircuitWorks[®] Conductive Epoxy from Chemtronics is a two part silver epoxy used in prototype, repair and general conductive bonding applications. This glue was chosen for its simple mixing ratio, excellent electrical conductivity, fast curing, high strength bond, and ability to bond dissimilar surfaces.



Fig.39: CircuitWorks[®] Conductive Epoxy from Chemtronics.

The Velostat squares were glued on the bottom layer with a multi-steps process:

- a mask was created for locating the right spots where apply glue along the copper lines: a transparent plastic sheet was drilled in 30 points and superimposed on the circuit. The holes were drilled by a diameter small enough to prevent too much glue fell on the circuit.

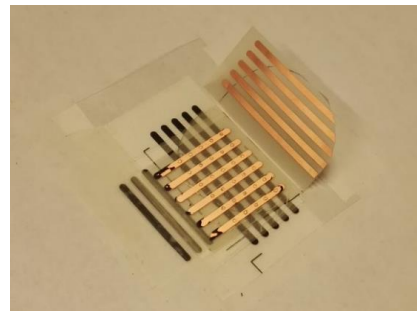
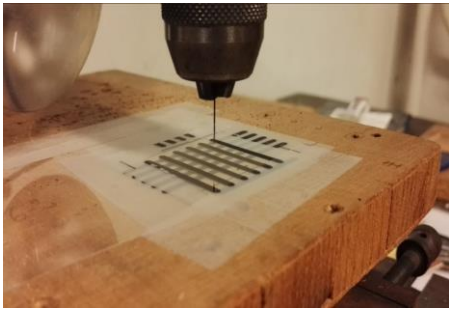


Fig40: Realization of the mask (left) and its positioning over the bottom layer of the sensor (right).

- The glue was prepared: It has a mixing time of 2 minutes;
- A thin sheet of glue was applied on the mask
- the mask was removed

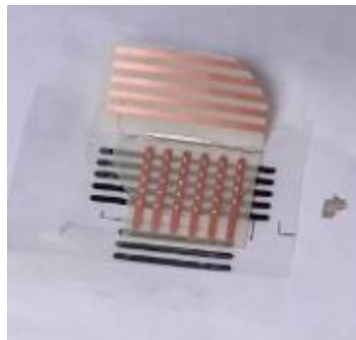


Fig:41 Bottom layer of the sensor after removing of the mask.

- the velostat squares were applied using tweezers: the procedure was made in 5 minutes, that is the curing time of the glue;
- The second layer was superposed and a 1kg weight was put on the closed sensor to permit a secure and uniform gluing. After 4 hours, the fixing procedure was completed.

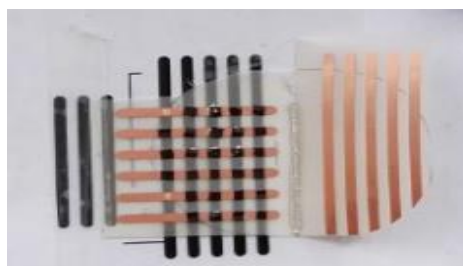


Fig.42: Bottom layer of the sensor after Velostat sensels gluing.

STEP 3: SOLDERING OF THE WIRES

To permit the link between the sensor and the DAQ, for each row and column a wire was soldered.

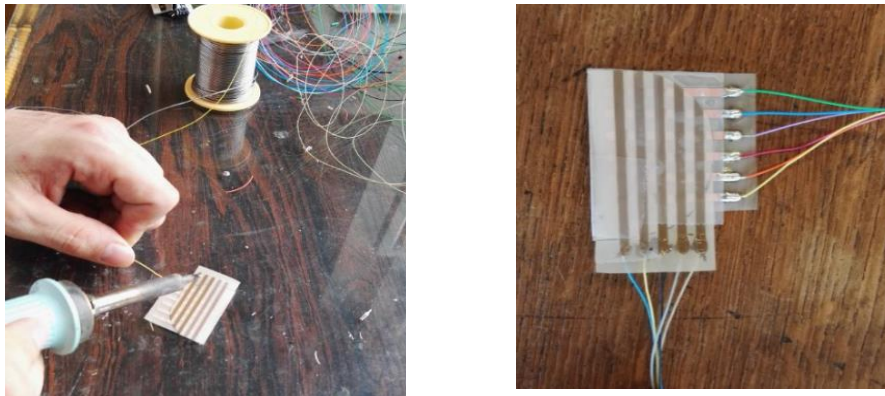


Fig.43: Soldering of the wires.

To verify the operating principle of the device, an instrumentation platform is necessary to power the circuit and to acquire, visualize and store its output signals.

PXI System is one of several modular electronic instrumentation platforms in current use. These platforms are used as a basis for building electronic test equipment, automation systems, machine monitoring and modular laboratory instruments.

PXI systems hardware are composed of three basic components -- chassis, controller, and peripheral modules.



Fig.44: PXI system.

The PXI chassis is the backbone of PXI system. It provides the power, cooling, and communication buses for PXI controller and modules. All PXI chassis contain a system controller slot located in the

leftmost slot of the chassis (slot 1). Embedded controllers eliminate the need for an external PC, therefore providing a complete system contained within the PXI chassis (stand-alone systems). There are several types of modules to be inserted in the slots: analog input/output, Digital input/output, Instruments, Receiver interconnect devices...

The development and operation of a Windows-based PXI or PXI Express system is no different from that of a standard Windows-based PC, application software or programming techniques are the same.

The BEAMS department of ULB owns a PXI System produced by National Instrument; the modular system is composed by a compact 8-slot chassis (NI PXI-1042) combined with an embedded controller (NI PXI-8106) and a multifunction data acquisition (DAQ) module (NI PXI-6224) with 32 analog inputs and 48 digital I/O lines (divided in two channels, Ch 0 and Ch 1). There is also an I/O connector block (PXI SCC-68) to connect the measurement system to the DAQ module, that features screw terminals and breadboard area for I/O signal connections.

NI PXI's hardware works together with Labview software, used to communicate with the hardware. LabVIEW programs are called virtual instruments, or VIs, because their appearance and operation imitate physical instruments, such as oscilloscopes or strain gauges or thermocouples. LabVIEW contains a comprehensive set of tools for acquiring, analyzing, displaying, and storing data, as well as tools to help the user troubleshoot code he writes.

In LabVIEW, is possible to build a user interface, or front panel, with controls and indicators.

PXI platform is expandable with specific modules for strain gauges output signals acquisition; in particular, the NI PXI-1042 chassis is compatible with the 2-Channels NI PXI-4220 module.

The manufactured load cell is composed of 4 wheastone bridges, so 4 acquisition channels are required, then 2 NI PXI-4220 modules.

If completed with strain gauge modules, the PXI system permit to write one single Labview code in which both the data from load cell and position sensor could be inserted and combined, to calculate and to visualize on the front panel of the the kinetics and kinematics of the prosthesis. Unfortunately, because of unexpected problems about the available budget for the project, after having received a quote from National Instrument, it has been not possible to buy the NI PXI-4220 modules for the calibration and testing of the load cell.

4. Testing and Results

Once realized the prototype, the aim of the thesis was accomplished: furthermore, it was interesting to put into practice the teoretical ideas about the position sensor, with the sole purpose of testing its functioning, getting qualitative results and understanding how to interpret its outputs.

The femoral component, tibial tray and tibial insert of the original prosthesis (Gemini SL PS Total knee prosthesis, Link) were 3D printed in the BEAMS Department to make the experimental pilot test. Befor to be printed, the CAD files were transferred on a software linked to the 3D printer. The 3D printer uses PLA as ink (Young modulus = 3.5 Gpa), which is melted and deposed on a glass base, through a nozzle with a diameter of 0.5mm, that determines the resolution of the printing. The development of the pieces is reached following a deposition of the PLA layer by layer, with a sponge structure inside (hexagonal cells) and a thick cover. The composition of the PLA can be regulated through the setting of different parameters: the density, the thickness of the cover and of the layers.

The first step for testing procedure, was to create the electrical circuit on a breadboard, in order to reproduce phisically the theorethical matrix of voltage dividers.

For both the medial and lateral position sensors there was need for:

- 5 electrical reference resistances R_r
- 6 digital switches

Before to start, the nominal resistance of Velostat foil was measured with a multimeter: whitout any pression it is 3Kohm, when pressed it values reduces up to 400 ohm. For this reason, reference resistances R_r of 3kOhm and a supply voltage of 5V were chosen for the circuit. The circuit has been mounted on a breadboard big enough to place both the medial and the lateral circuit components. The power supply and the reference ground of the circuit are provided by PXI analog outputs pins and connected to power rails of the breadboard (red and blue horizontal lines, Fig.45) The vertical equipotential lines correspond to the columns of the matrix: each of these columns acts as a voltage divider and their output voltages are withdrawn and directed to the PXI Analog Input pins.

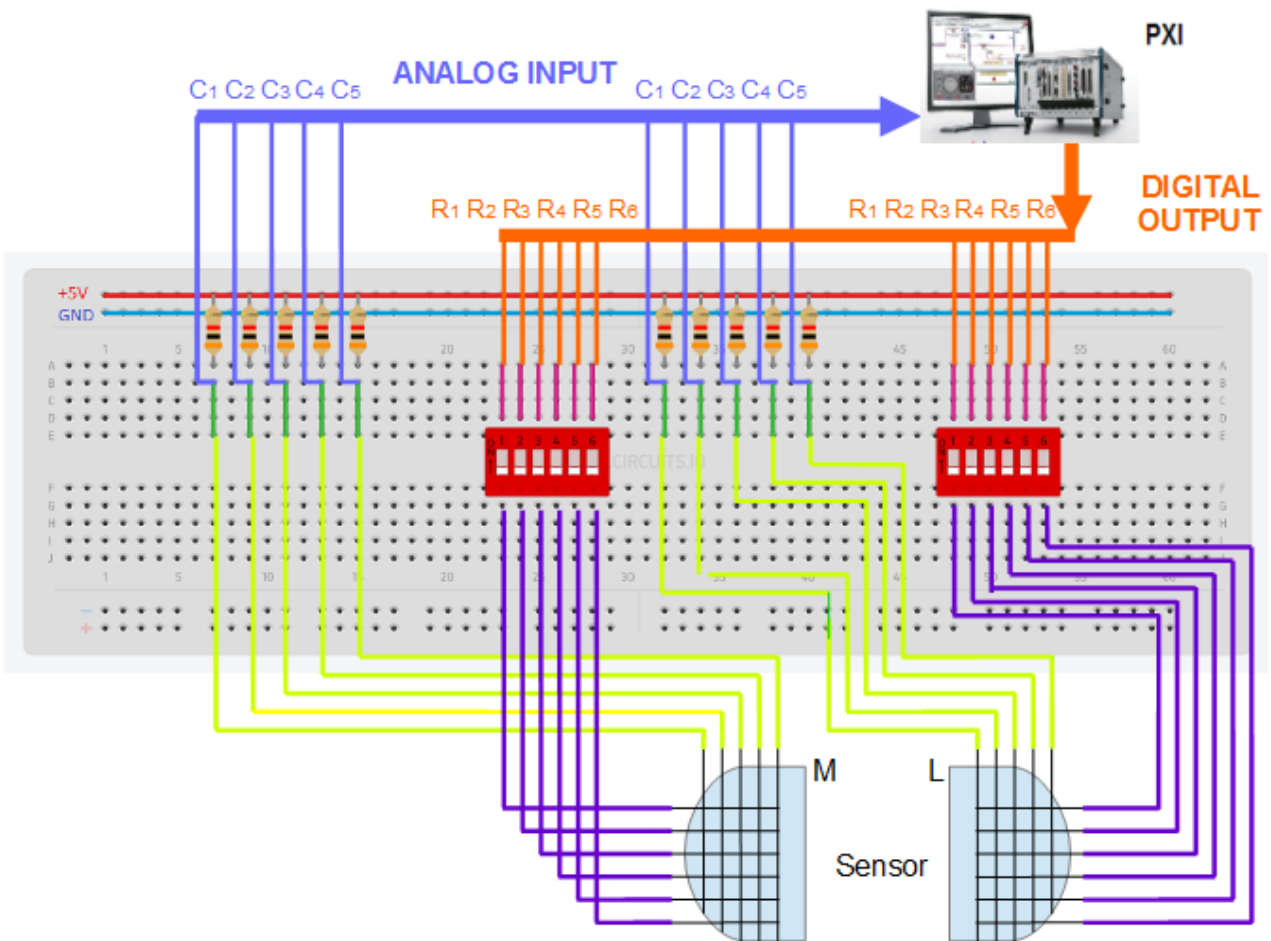


Fig. 45: Schematic view of the circuit on the breadboard.

The activation of each row is made by the ULN2803A Darlington Transistor Array (Texas Instrument): it consists of eight NPN Darlington pairs, one for each pin of the device.



Fig. 46: ULN2803A Darlington Transistor Array (Texas Instrument).

When the base of the NPN transistor is grounded, no current flows from the emitter to the collector and the transistor is therefore switched "OFF". If the base is forward biased by more than 0.7 volts, a current will flow from the emitter to the collector and the transistor is said to be

switched "ON". When operated in these two modes, each transistor of the array is a switch. So, each base of the array is connected to the digital output generated by the DAQ, each collector output is connected to a row of the sensor.

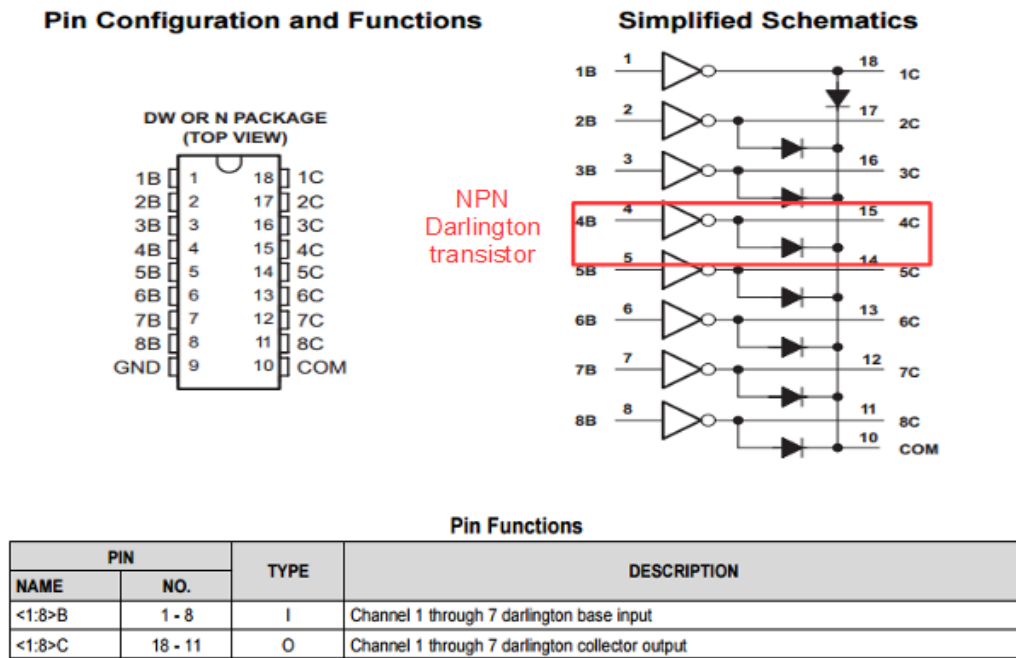


Fig. 47: ULN2803A Darlington Transistor Array (Texas Instrument): pin configuration and function, from datasheet.

There are two possible states for each row:

- "true" digital output = switch "ON" (closed) = row activated (connected to the ground)
- "false" digital output = switch "OFF" (open) = row deactivated (open circuit)

The digital outputs of the DAQ has been controlled via software: a Labview code generates the sequential turning on of the rows.

The connector block SCC-68 acts as a bridge between the PXI and the sensor, so it was connected to the Ch1 of the NI PXI-6224: Each screw terminal on its breadboard corresponds to one pinout of the DAQ, so for each compartment of the sensor were selected:

- 5 Analog input (AI) pinouts for reading the voltage outputs of voltage dividers;
- 6 Digital output (DO) pinouts for activating the rows;
- 5V analog output (AO) pinouts for power supply;
- Digital Ground output (D GND) pinouts as references for the signals.

In Fig.48 is shown the realized circuit connected to SCC-68; 10 AI and 12 D I/O pinouts were used, so it was sufficient to use only one channel (Ch1) of the NI PXI-6224 module.

The Labview code for controlling the circuit and acquiring the data is reported in the Appendix D.

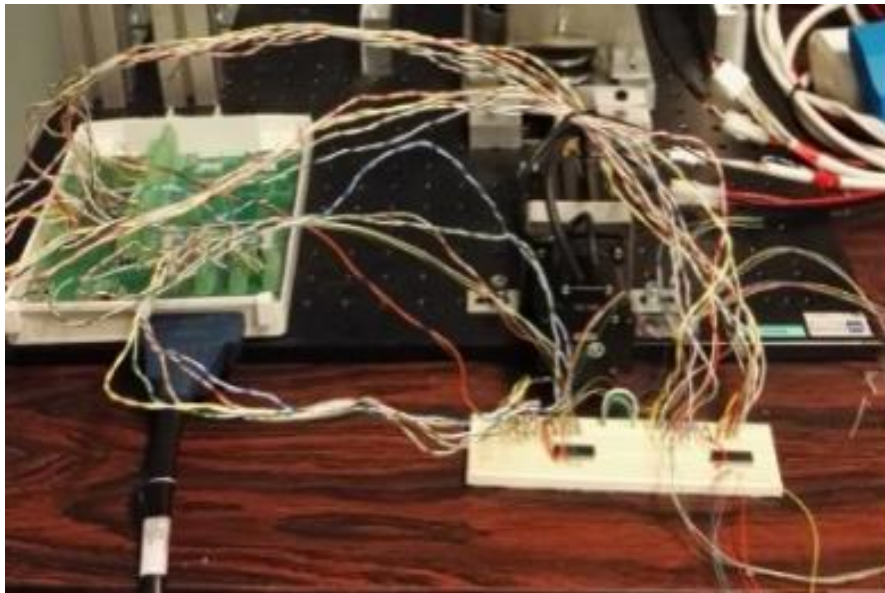
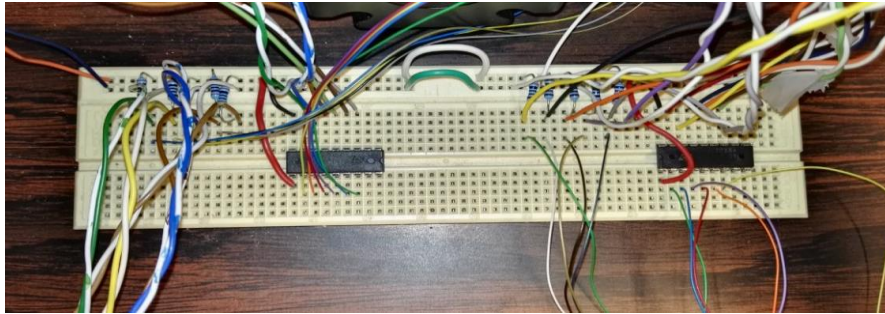


Fig. 48: Breadboard (Up). Breadboard connected to the SCC-68 connector block (Down).

The Labview program has been written for showing dynamically the results of the acquisition, in both numerical and graphical way.

In fact, once turned on the power supply of the circuit and began the acquisition, the front panel of the Labview software displays simultaneously the acquisition matrix of both medial and lateral sensors and their graphical transposition in a 2D-graph, where the x-axis reports the rows of the matrix, the y axis the columns, numbered from 0 to n-1, where n is the number of lines.

Each x-y-point (pixel) of the 2D-Graph corresponds to a sensel of the position sensor. As shown in the colormap, the color intensity of a pixel is inversely proportional to the corresponding numeric

tension values.

The front panel also displays the y-x-coordinates of the contact point, that is the darkest pixel (the sensel with the lower tension output): this coordinates are useful to calculate the displacement of the contact point from one position to another during the experimental tests. (Fig.49)

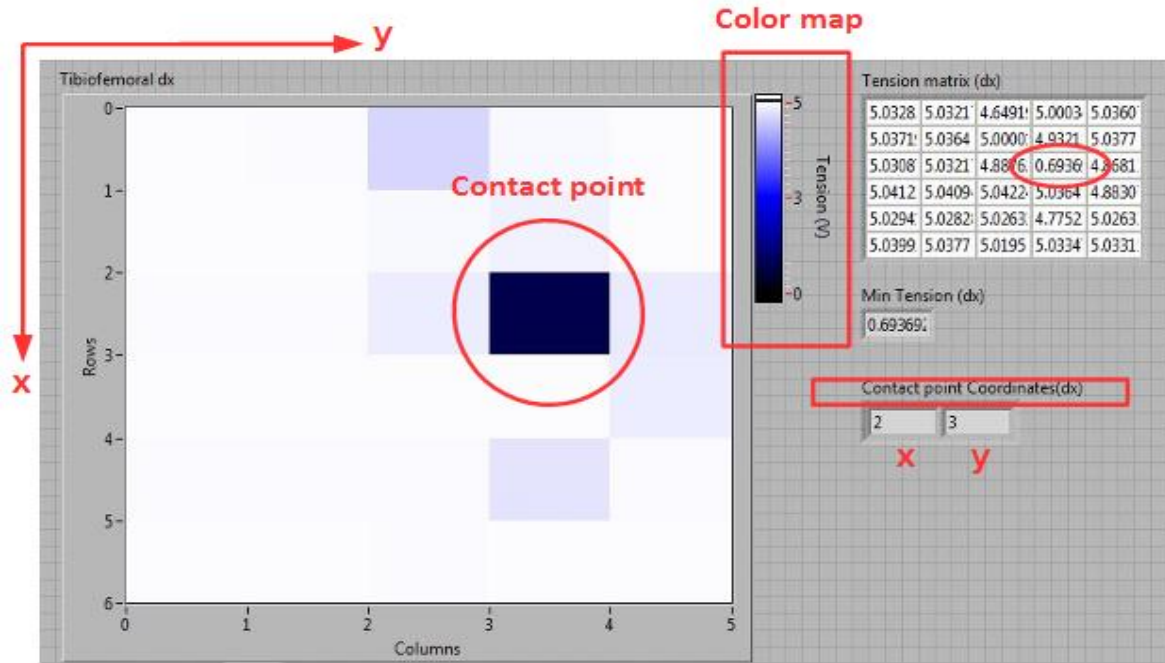


Fig.49: Frontal panel of Labview program during an acquisition test.

Before testing the sensor inside the prosthesis, it was considered appropriate to start from the simplest tests. The sensor was pasted on a flat surface and moving the finger on the top layer, its motion was dynamically followed on the front panel of the PXI System. (Fig.50)



Fig. 50: First test on a flat surface.

The sensor responded well to these first tests, as the movements of contact point displayed on the front panel matched those of the finger.

Given this positive response, the medial and the lateral sensors were glued on the 3D printed tibial insert plateaus, to make additional tests in more realistic conditions.

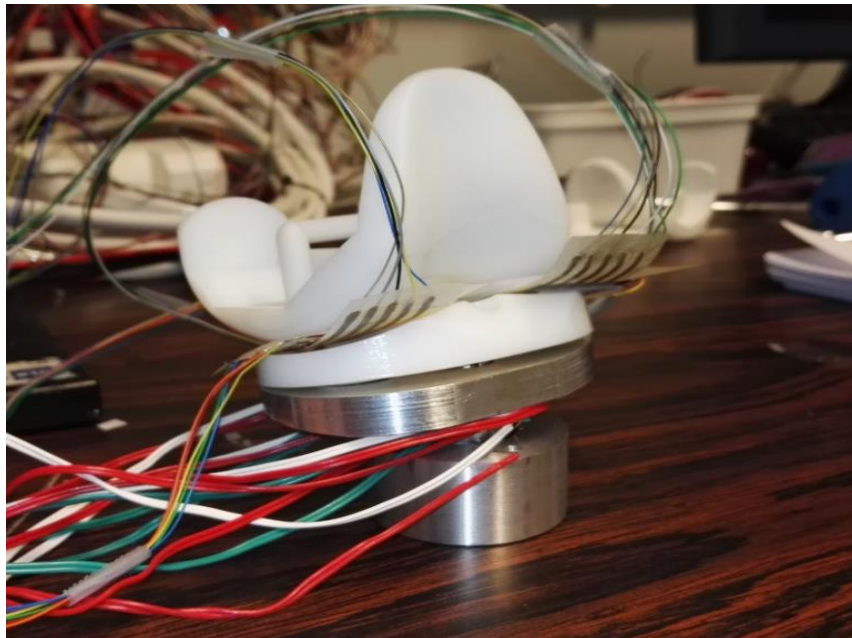


Fig.51: Pilot test on instrumented prosthesis.

The insert was mounted on the tibial tray of the prototype, and a simple movement of flexion-extension was simulated rotating the femoral component in the sagittal plane from 0° up to 90° , following the movement of the sensor on the frontal panel.

Fig.52 shows the outputs of the labview code for the medial and the lateral compartments, acquired in four steps of rotation: 0° - 30° - 60° - 90° .

It should be noted that these results are not comparable with kinematics data from literature, as the movement simulated during testing is not physiological. However the kinematic analysis of the prosthesis was outside the scope of the thesis, then the test was done for a qualitative analysis of movements and to find, within the limits imposed by the resolution, a calculation procedure of displacement.

MEDIAL COMPARTMENT

LATERAL COMPARTMENT

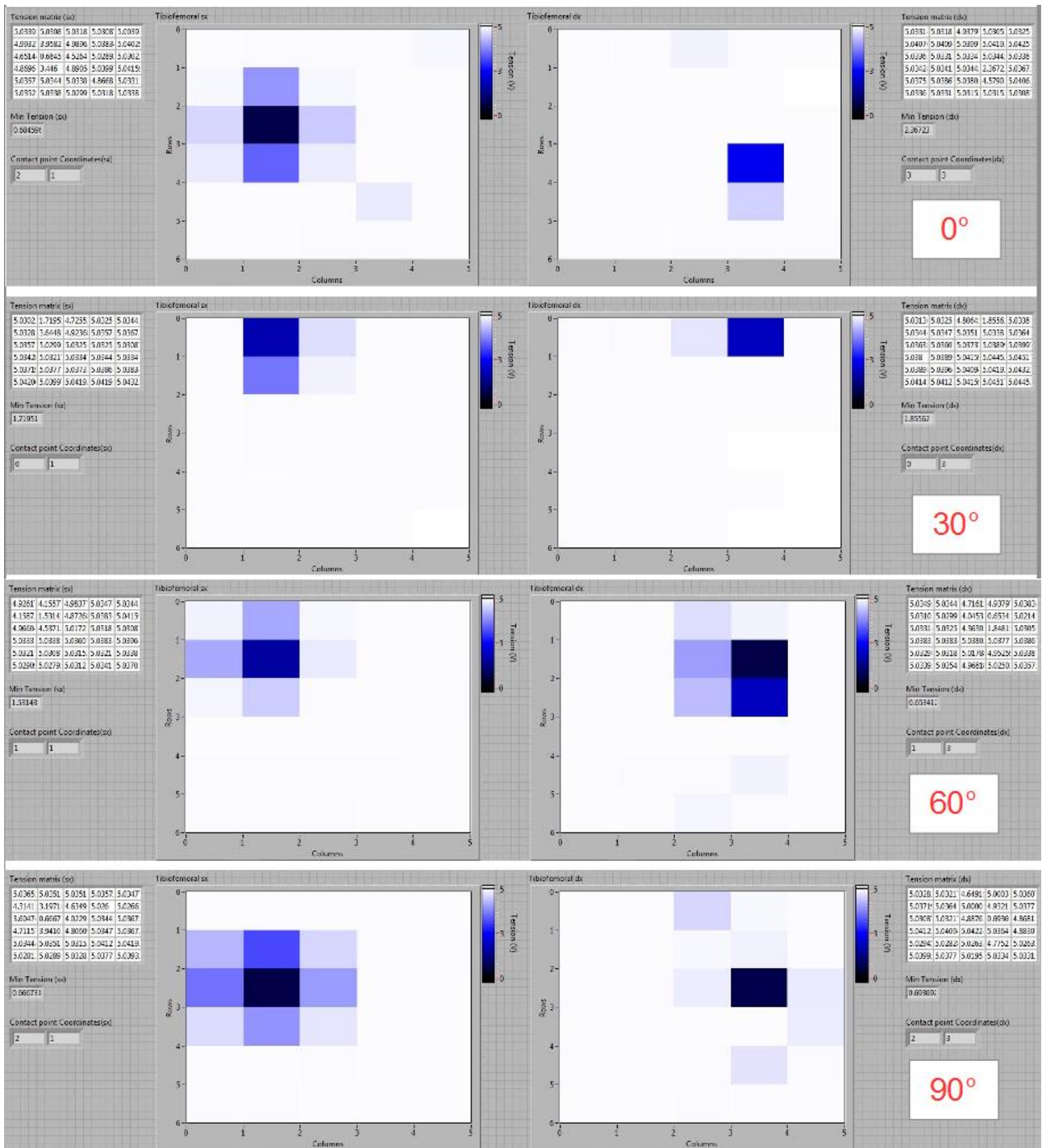


Fig.52: Contact points of femoral component in the medial and the lateral compartment in 4 steps of flexion-extension movement (0°-30°-60°-90°). During the test, from one step to the other, front panel showed dynamically the movements of the contact points and the x-y coordinates.

As explained in the previous chapter, the sensor is composed by 30 square-shaped sensitive elements, 2mm side; it has a resolution of 6 sensitive elements/cm².

This means that each element of the acquisition matrix in the 2D Labview graph corresponds to a rectangular sensel (4x5mm) on the sensor. Then, each measurement value is accompanied by an uncertainty: $\pm 2\text{mm}$ along the y axis and $\pm 2.5 \text{ mm}$ along the x-axis. (Fig.52)

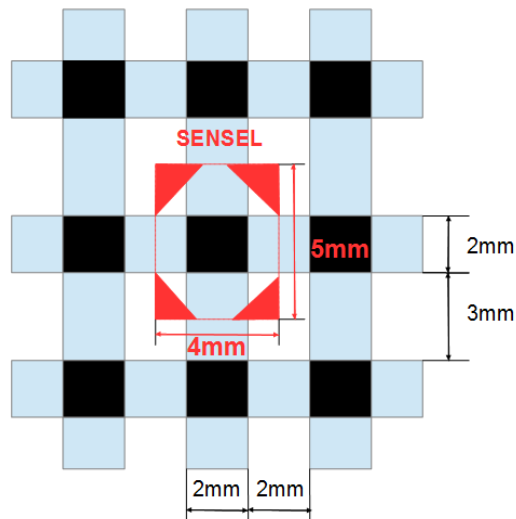


Fig.52: Magnified view of the sensor matrix. (Particular)

To measure the displacement of the femoral component between different positions, it is useful to represent the results in a more immediate way, simply projecting the position sensor on the tibial insert and reporting the resultant contact points on the projected sensels.

Fig. 53 shows the projected results on the tibial insert, for each of the four steps of the flexion-extension movement, from 0° to 90°.

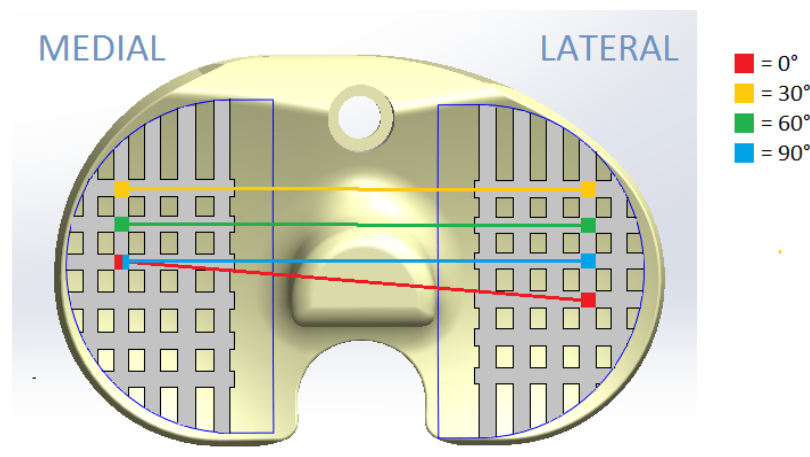
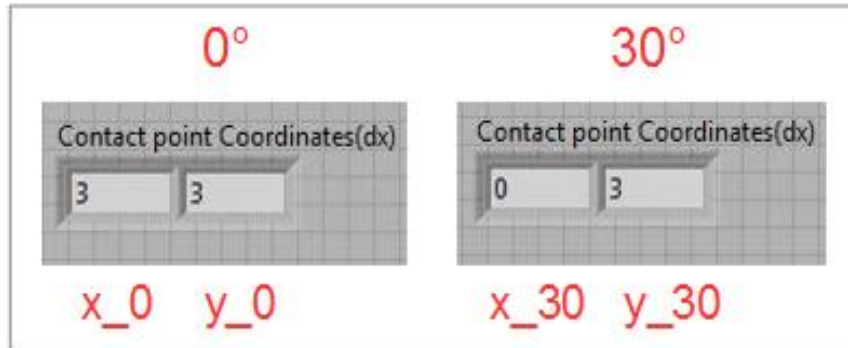


Fig.53: Projection of the contact points on the tibial insert surface, during 4 steps of flexion extension.

Consider as example the biggest movement of the femoral component, observed in the lateral compartment after the first step of rotation (0°-30°).

The two contact points x-y coordinates are:



So the contact point stayed still in the y direction and moves three sensels in the x direction: each sensel is 5mm side, so the total displacement is 15mm.

This value must be considered with an uncertainty of 5 mm, the sum of the uncertainties of the contact points. So, the displacement of the femoral component is (15 ± 5) mm in AP direction and (0±5) mm in ML direction.

Improving the resolution of the sensor most reliable values can be achieved by implementing the same simple procedure.

Another interesting demonstration was to test a modified sensor, in which the second layer was a whole Velostat foil. The results shown in Fig. 54 demonstrate that, as predictable, measuring becomes even more inaccurate, because of parasitic resistances between the lines.

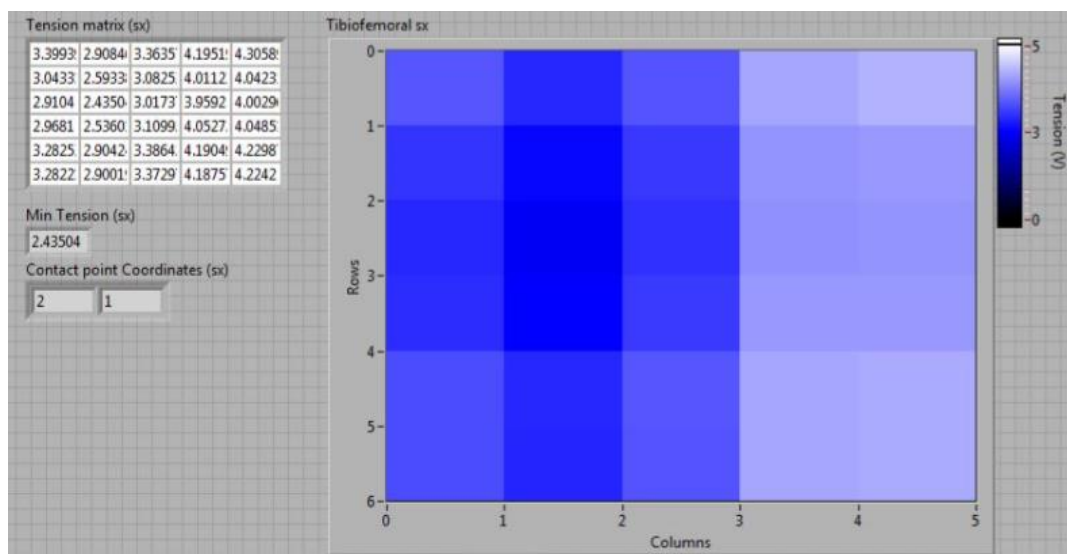


Fig.54: Front panel during a test with modified sensor.

5. Discussions and future perspectives

The position sensor designed in this project represents the first documented attempt to manufacture a low cost device for the study of knee kinematics, that aims to overcome the limits of the methods normally used as the inaccurate gait analysis, the invasive fluoroscopy and the fragile Tekscan system. In particular, there was designed a three-layers piezoelectric sensor with an operating principle similar to the Tekscan one, but aimed at higher performances, lower costs, and more easily synchronizable with kinetic data obtained from load cell.

The pilot test allowed to put into practice the theoretical idea about the sensor and to analyze its manufacturing problems, advantages, limitations and room for improvement: all these information are the basis upon which to make future experimental tests and improve the prototype.

At this preliminary stage of the project in fact, it would be useless to test the sensor simulating physiological knee movement on a robotic knee simulator, the results are not acceptable.

In fact, the resolution of the manufactured prototype does not meet the desired specifications, because it is even lower than those of the experimental methods used so far. As previous explained, the sensels size is $(4 \times 5) \text{ mm}^2$, about twice that of Tekscan's sensels, so the two methods are not yet comparable.

However it has to be considered that the sensor resolution has been chosen deliberately so low to ease the process of implementation and avoid unnecessary complications and delays during the manufacturing process. The advantage of this sensor is that, unlike the Tekscan system, resolution can be improved: laser machinery for printing circuit boards present in BEAMS Department in fact, can print copper tracks up to 0.1 mm thick, greatly reducing the size of the sensels.

So, in the next tests, the lines will be printed thinner and closer together to limit the interlines space and improve the measurement resolution.

This process should be done gradually, as the increase in the number of tracks and the decrease of their thickness can easily cause problems in the practical implementation of the circuit, as the increase in the number of wires inside the experimental setup. However the sensor is not supposed to be used in vivo: so, this issue is not particularly significant. Alternatively, to avoid the redundancy of the tracks, it could be done an high resolution sensor with reduced sensing area: it will not cover the entire surface of the tibial plateau, but it may be located in different areas depending on the movement to be studied.

An increased resolution would require even more refined and accurate materials and machinery for the practical implementation of the sensor, in fact during the pilot test were discovered some limitations in making the sensor within a research laboratory:

- the plastic substrate material of the printed circuits (upper and bottom layers) tends to melt with the heat of welding wires;
- Velostat squares can be glued on one side only: a sticking too tight between the two layers can flex the piezoresistive foil that, being very sensitive, reduces its nominal resistance at rest, altering the accuracy of measurement;
- the sensor is too sensitive to short circuit: just using too much glue, or in the presence of small inaccuracies in placement or in the form of the sensels, the conductive tracks of the upper and bottom layers can become in contact;
- the DAQ has proved to not have an instantaneous response, because the data appeared on the screen with slight delay.

These limitations have considerably slowed down and hindered the process of realization, which was repeated three times because of the rupture of the sensor or short circuits; however, they are strictly due to the manufacturing tools and not to the basic idea of the sensor, so they are definitely fixable. For example, for the next tests it should be better to choose a glue with higher strength bond (to avoid using too much causing short circuit) and reduced drying time, to paste the sensels in a more careful and unhurried way. Furthermore, reducing the thickness of the copper circuit traces and increasing their number, will be necessary to use a more accurate system for welding and cutting the sensels.

In conclusion, despite the difficulties encountered in its implementation, the sensor has responded well to pilot test: it has resisted well to roto-translation of the femoral component and it was able to follow its movements without damages during the test.

Furthermore, despite the foreseeable limits, the test produced meaningful results. Looking at the point of contact in both compartments of the tibia in fact, it is possible to do some qualitative considerations. It is clear that during a simple flexion-extension simulation, the contact point moves only in the anteroposterior direction in both compartments, but asymmetrically: the displacement in the lateral compartment are much wider than in the medial one. This information,

although only qualitative, is a very satisfactory result. In fact, until now no instrumented implants can measure kinematic data directly, but these are recorded by external devices.

In particular, the research group of D'Lima, in both uniaxial and multi-axial prototype, obtained kinematic data using dual fluoroscopic imaging system, testing the instrumented implant both in vivo and in vitro. Although this technique can be accepted for in vitro experiments, has no prospects of using in vivo because it is very invasive, and often proved inaccurate. Furthermore, with this technique is not possible to obtain kinematics data dynamically and real-time, so the distribution of tibio-femoral force between the two compartments can be obtained only by a post-processing of stored data. Bergmann et al. used the gait analysis to calculate the kinematics of instrumented implants during in vivo tests: also this technique proves to be not suitable for accurate results, because the error due to the movement of the markers gives a resolution even comparable to that of the sensor made in this project.

In the next step of the project, the PXI configuration will be completed with modules for the acquisition of strain gauges. This will allow the completion of the Labview code: in the same acquisition program kinematic data can be displayed, stored and processed instantaneously and simultaneously to force data providing, as real-time output, the percentage of tibio-femoral force distribution, without further post-processing.

Before to test the device on knee simulator, a calibration of load cell will be needed. The load cell is designed to measure four loading components: one axial load, two orthogonal bending moments and one torsional moment, so four different types of calibration tests must be performed. For each test the transducer must be mounted on a loading jig and loaded according to the sensing direction, to obtain four different calibration matrix. For each type of loading component or motion task, it would be better to calibrate the load cell with the range of values reported in the literature, to optimize its sensitivity.

After the tibio-femoral tests, the next step will be to realize the patellofemoral component, calibrate its load cell, and fix the mounting block on the robotic Simulator with specific mounting stripes.

Once completed, the device will be mounted on the knee simulator of the BEAMS department allowing to test different interchangeable designs of prostheses during several motor tasks.

6. Conclusions

The main goal of the project was to design an instrumented customizable total knee implant for the measurement of the internal knee kinetics (in terms of medial and lateral forces, patello-femoral forces) and kinematics during experimental tests on robotic knee simulator.

Such tool was designed not aimed for an industrial application but focusing on research application. For this reason, the implant was planned to be customizable, i.e. able to investigate the knee behaviour induced by different design features (as different Post-Cam design or position, change in the condylar radius, change in the prosthesis design etc.).

The device was created modifying the structure of a commercial prosthesis: the tibial tray became a modular multi-axis load cell, whose cylindrical sensing element is fixed on knee Simulator in the bottom side, and screwed to an interchangeable top plate, housing the polyethylene insert, in the upper side. This mechanism permits to easily test different prosthesis designs.

As regard the patello-femoral joint, it was designed a structure that works not only as mounting block for knee robotic Simulator, but also as a support for the load cell, which is identical to that of the tibio femoral joint and mounted on the posterior part of patellar insert.

For monitoring the kinematics of the femoral component a three-layer, piezoelectric position sensor was manufactured in BEAMS department, using a Velostat foil.

This sensor, designed with the aim to overcome the limitations of Tekscan system, so far used in the BEAMS laboratory, has responded well to pilot test: using a PXI platform present in BEAMS department it was possible to graphically follow the movements of the femoral component and identify the coordinates of its contact point on the tibial insert through a Labview program.

The device has shown great room for improvement and, increasing resolution, may represent a viable alternative to the Tekscan sensor.

Kinetic and kinematic data can be acquired with the same PXI platform and combined mathematically to split medial and lateral tibio-femoral force. The forces can then be displayed and stored in real time, without the need for post-processing.

All the work was also performed at very low cost, buying only the conductive glue needed to assembly the layers of the sensor.

The aim of the thesis was then fully achieved: in the later stages of the project it will be possible to calibrate the load cell and carry out the first tests on knee Simulator, combining the kinetic and

kinematic data.

Such device can be helpful for clinicians, engineers and researchers.

In fact it can be used to validate existing numerical models of the knee and of TKA and create new ones, more accurate.

It can lead to refinement of surgical techniques, to enhancement of prosthetic designs and to design more effective in vitro knee testing rigs and knee wear simulators.

Once validated, and if properly modified, an additional use of this device could be intraoperative measurement of forces to determine soft tissue balancing, evaluation of the effects of rehabilitation, external bracing, and activities more vigorous than those of daily living (such as athletic and recreational activities).

Given the current increase in the number of older persons who are at higher risk for chronic musculoskeletal disorders, and therefore of knee prosthesis, a significant positive impact on clinical outcomes and patient health care could be also anticipated as possible benefit of this research project.

7. Bibliography

1. Goldblatt J, MD, Richmond J, MD. Anatomy and biomechanics of the knee. *Operative Techniques in Sports Medicine*, Vol 11, No 3 (July), 2003: pp 172-186.
2. Bellemans J, Ries MD, Victor J. Total Knee Arthroplasty, A Guide to Get Better Performance. *Springer*, Germany, 2005.
3. Masouros SD, Bull AM, Amis AA. Biomechanics of the knee joint. *Orthopaedics and Trauma*, 24(2):89-91, 2010.
4. Kuster M, Wood G, Stachowiak G, Achte A. Joint load considerations In Total Knee Replacement. *J Bone Joint Surg [Br]* 1997;79-B:109-13.
5. Bellemans J, Vandenneucker H, Vanlauwe J. Total knee replacement (iv). *Current Orthopaedics* (2005) 19, 446-452.
6. Jacobs W, Anderson PG, van Limbeek J, Wymenga AAB. Mobile bearing vs fixed bearing prostheses for total knee arthroplasty for post-operative functional status in patients with osteoarthritis and rheumatoid arthritis (Review). *TheCochrane Library* 2001, Issue 2.
7. Fricka KB, Sritulanondha S, McAsey C. To cement or not? Two-Years Results of a Prospective, Randomized Study Comparing Cement Vs. Cementless Total Knee Arthroplasty (TKA). *The Journal of Arthroplasty* 30 Suppl. 1 (2015) 55-58.
8. Kurtz S, Ong K, Lau E, Mowat F, Halpern M. Projections of primary and revision hip and knee arthroplasty in the United States from 2005 to 2030. *J Bone Joint Surg Am.* 2007 Apr;89(4):780-5.
9. Nguyen L, Lehil M, Bozic K. Trends in Total Knee Arthroplasty implant utilization. *The journal of Arthroplasty* 30 (2015) 793-742.
10. Kurtz S, Lau E, Ong K, Zhao K, Kelly M, Bozic K. Future young patient demand for Primary and Revision joint replacement. *Clin Orthop Relat Res* (2009) 467:2606-2612.
11. Julin J, Jamsen E, Puolakka T, Konttinen YT, Moilanen T. Younger age increases the risk of early prosthesis failure following primary total knee replacement for osteoarthritis. a follow-up study of 32,019 total knee replacements in the Finnish Arthroplasty Register. *Acta Orthop.* 2010; 81:413-9.
12. Kyung T K, Song Lee, Dong Oh Ko, Bong Soo Seo, Jung WS, Chang BK. Causes of Failure after Total Knee Arthroplasty in Osteoarthritis Patients 55 Years of Age or Younger. *Knee Surg*

13. Victor J. Rotational alignment of the distal femur: A literature review. *Orthopaedics & Traumatology: Surgery & Research*. Volume 95, Issue 5, September 2009, Pages 365–372
14. Bourne R, Chesworth B, Davis A, Mahomed N, Charron K. Patient Satisfaction after Total Knee Arthroplasty. Who is Satisfied and Who is Not? *Clin Orthop Relat Res* (2010) 468:57–63
15. Morrison JB. The mechanics of the knee joint in relation to normal walking. *J Biomech*, 1970. 3:51–61
16. Seireg A, Arvikar RJ. A mathematical model for evaluation of forces in lower extremities of the musculo-skeletal system. *J Biomech*, 1973.6:313–326
17. Benoita D, Ramseyd D, Lamontagne M, Xuf L, Wretenberg Per, Renströma P. Effect of skin movement artifact on knee kinematics during gait and cutting motions measured in vivo. *Gait & Posture*. Volume 24, Issue 2, October 2006, Pages 152–164.
18. Catani F, Innocenti B, Belvedere C, Labey L, Ensini A, Leardini A. The Mark Coventry Award: Articular Contact Estimation in TKA Using In Vivo Kinematics and Finite Element Analysis. *Clin Orthop Relat Res* (2010) 468:19–28.
19. Taylor W, Heller M, Bergmann G, et al. 2004. Tibio-femoral loading during human gait and stair climbing. *J Orthop Res* 22:625–632.
20. Kuster MS, Wood GA, Stachowiak GW, et al. 1997. Joint load considerations in total knee replacement. *J Bone Joint Surg Br* 79:109–113.
21. Shelburne KB, Torry MR, Pandy MG. 2005. Muscle, ligament, and joint-contact forces at the knee during walking. *Med Sci Sports Exerc* 37:1948–1956
22. Mikosz RP, Andriacchi TP, Andersson GB. 1988. Model analysis of factors influencing the prediction of muscle forces at the knee. *J Orthop Res* 6:205–214.
23. Seireg A, Arvikar RJ. 1975. The prediction of muscular load sharing and joint forces in the lower extremities during walking. *J Biomech* 8:89–102.
24. Pianigiani S, Labey L, Pascale W, Innocenti B. Knee kinetics and kinematics: What are the effects of TKA malconfigurations? *Knee Surgery, Sports Traumatology, Arthroscopy*. (2015) pp 1-7
25. Pianigiani S, Chevalier Y, Labey L, Pascale V, Innocenti B. Tibio femoral kinematics in different total knee arthroplasty designs during a loaded squat: A numerical sensitivity

- study. *Journal of Biomechanics* 45 (2012) 2315–2323
26. Innocenti B, Pianigiani S, Labey L, Victor J, Bellemans J. Contact forces in several TKA designs during squatting: A numerical sensitivity analysis. *Journal of Biomechanics*. Volume 44, Issue 8, 17 May 2011, Pages 1573–1581
 27. Chapman-Sheath PJ, Bruce WJM, Chung WK, Morberg P, Gillies RM, Walsh W.R. In vitro assessment of proximal polyethylene contact surface areas and stresses in mobile bearing knees. *Medical Engineering & Physics* 25 (2003) 437–443.
 28. Innocenti B, Bilgen OF, Labey L, van Lenthe H, Vander Sloten J, Catani F. Load Sharing and Ligament Strains in Balanced, Overstuffed and Understuffed UKA. A Validated Finite Element Analysis. *The Journal of Arthroplasty* 29 (2014) 1491–1498
 29. Luyckx T, Didden K, Vandenneucker H, Labey L, Innocenti B, Bellemans J. Is there a mechanical explanation for anterior knee pain in patients with patella alta? *J Bone Joint Surg [Br]* 2000;91-B:344-50.
 30. Didden K, Luyckx T, Bellemans J, Labey L, Innocenti B, Vandenneucker H. Anteroposterior positioning of the tibial component and its effect on the mechanics of patellofemoral contact. *J Bone Joint Surg [Br]* 2010;92-B:1466-70.
 31. Kuwashimaa U, Hamaia S, Okazakia K, Satorulkebeb, Higakib H, Mizu-uchia H, Akasakia Y, Murakamia K, Yukihidelwamotoa. Contact stress analysis of the anterior tibial post in bi-cruciate stabilized and mobile-bearing posterior stabilized total knee arthroplasty designs. *Journal of the mechanic behavior of biomedical materials* 60 (2016) 460–467
 32. Arnout N, Vanlommel L, Vanlommel J, Luyckx JP, Labey L, Innocenti B, Victor J, Bellemans J. Post-cam mechanics and tibiofemoral kinematics: a dynamic in vitro analysis of eight posterior-stabilized total knee design. *Knee Surg Sports Traumatol Arthrosc* (2015) 23:3343–3353
 33. Bachus KN, DeMarco AL, Judd KT, Horwitz DS, Brodke DS. Measuring contact area, force, and pressure for bioengineering applications: Using Fuji Film and TekScan systems. *Medical Engineering & Physics* 28 (2006) 483–488
 34. Burny, F., Moulart, E. and Bourgios, R. Mesure de la deformation des implants ‘in vivo’. Resultats dune etude partant sur dix patients traités par clau-plaque. *Actu Orp. Belg.* (Supp 1) (1976) 42, 52-61.
 35. Nunamaker, D. M. and Perren, S. M. Force measure- ments in screw fixation. *J.*

- Biomechanics* 9 (1976), 669-675.
36. Rydell, N. W. Forces acting in the femoral head prosthesis. *Acta Orthop Scand* (Supp. 88) (1966) 37, 1-132.
 37. Taylor SJ, Walker PS, Perry JS, et al. The forces in the distal femur and the knee during walking and other activities measured by telemetry. *J Arthroplasty* (1998).13:428–437
 38. Kaufman K, Kovacevict N, Irby S, Colwell C. Instrumented Implant For Measuring Tibiofemoral Forces. *J Biomechanics*. Vol. 29, (1996) No 5. pag 667-671
 39. Nicholls R, Schirm A, Jeffcote B, Kuster M. Tibiofemoral Force following Total Knee Arthroplasty: Comparison of Four Prosthesis Designs In Vitro. *J Orthop Res* (2007) 25:1506–1512.
 40. D. D’Lima D, Townsend CP, Arms SW, Morris BA, Colwell Jr CW. An implantable telemetry device to measure intra-articular tibial forces. *Journal of Biomechanics* 38 (2005) 299–304
 41. Morris BA, D’Lima D, Slamin JE, Kovacevic N, Arms SW, Townsend C, Colwell Jr CW. e-Knee: Evolution of the electronic knee prosthesis: Telemetry technology development. *J Bone Joint Surg Am*. (2001) 83-A Suppl 2:62-66.
 42. Mundermann A, Dyrby CO, D’Lima DD, Colwell Jr. CW, Andriacchi TP. In Vivo Knee Loading Characteristics during Activities of Daily Living as Measured by an Instrumented Total Knee Replacement.
 43. Zhao D, Banks SA, D’Lima DD, Colwell Jr. CW, Fregly B. In Vivo Medial and Lateral Tibial Loads during Dynamic and High Flexion Activities. *Journal of orthopaedic research*. (2007)
 44. Kirking B, Krevolin J, Townsend C, Colwell Jr. CW, D’Lima DD. A multiaxial force-sensing implantable tibial prosthesis.
 45. D’Limaa DD, Patila S, Steklova N, Chienb S, Colwell Jr CW. In vivo knee moments and shear after total knee arthroplasty. *Journal of Biomechanics* 40 (2007) S11–S17
 46. Varadarajana KM, Moynihana AL, D’Lima DD, Colwell Jr CW, Lia G. In vivo contact kinematics and contact forces of the knee after total knee arthroplasty during dynamic weight-bearing activities. *Journal of Biomechanics* 41 (2008) 2159–2168
 47. Fregly BJ, Besier Tf, Lloyd DG, Delp SL, Banks A, Pandy MG, D’Lima DD. Grand Challenge Competition to Predict In Vivo Knee Loads. *J Orthop Res* 30:503–513, 2012
 48. Heinlein B, Graichen F, Bender A, Rohlmann A, Bergmann G: Design, calibration and pre-clinical testing of an instrumented tibial tray. *J Biomech*. 40. S4–S10, 2007.

49. Bergmann G, Bender A, Graichen F, Dymke J, Rohlmann A, Trepczynski A, Heller MO, Kutzner I. Standardized Loads Acting in Knee Implants. PLOS ONE www.plosone.org (2014) Vol 9, Issue 1
50. Kutzner I, Heinlein B, Graichen F, Bender A, Rohlmann A, Halder A, Beier A, Bergmann G. Loading of the knee joint during activities of daily living measured in vivo in five subjects. *Journal of Biomechanics* 43(2010)2164–2173
51. Arami A, Simoncini M, Atasoy O, Ali S, Hasenkamp W, Bertsch A, Meurville Tanner S, Renaud P, Dehollain C, Farine PA, Jolles MB, Aminian K, Ryser P. Instrumented Knee Prosthesis for Force and Kinematics Measurements. *IEEE transactions on automation science and engineering*. (2013) vol. 10, no. 3.

8. Appendix

A – Load cells datasheets

3-Component Quartz Force Sensor (Kistler)

3-Component Quartz Force Sensor

16,5x16,5x10 mm, -3 ... 3 kN

Types 9017C, 9018C,
9016C4

Range	F_x, F_y	kN	-1,5 ... 1,5 ¹⁾
	F_z	kN	-3 ... 3 ¹⁾
	F_z	kN	0 ... 12,5 ²⁾
Overload	F_x, F_y	kN	-1,8/1,8 ¹⁾
	F_z	kN	-3,6/3,6 ¹⁾
Calibrated range	F_x	kN	0 ... 1,5 ¹⁾
	F_y	kN	0 ... 1,5 ¹⁾
	F_z	kN	0 ... 3 ¹⁾
	F_z	kN	0 ... 12,5 ²⁾
Permissible moment loading	M_x, M_y	N·m	-6,6/6,6 ¹⁾
	M_z	N·m	-6,6/6,6 ¹⁾
Threshold		N	<0,01
Sensitivity	F_x, F_y	pC/N	≈-25 ¹⁾
	F_z	pC/N	≈-11 ¹⁾
Linearity incl. hysteresis, each axis		%FSO	≤±0,5 ¹⁾
Crosstalk	$F_z \rightarrow F_x, F_y$	%	≤±1,0 ¹⁾
	$F_x \leftrightarrow F_y$	%	≤±2,5 ¹⁾
	$F_x, F_y \rightarrow F_z$	%	≤±2,5 ^{1) 3)}
Operating temperature range		°C	-40 ... 120
Insulation resistance at 20 °C		Ω	>10 ¹³
Ground isolation		Ω	>10 ⁸
Axial stiffness		N/μm	≈1 400
Shear stiffness		N/μm	≈300
Connector			V3 neg.
Weight		g	14



KISTLER
measure. analyze. innovate.

3- Component ICP Force Sensor (PCB Piezotronics)

Model Number	3-COMPONENT ICP® FORCE SENSOR	
260A01		
Performance	ENGLISH	SI
Sensitivity(± 20 %)(z axis)	2.5 mV/lb	0.56 mV/N
Sensitivity(± 20 %)(x or y axis)	10 mV/lb	2.25 mV/N
Measurement Range(z axis)	1000 lb	4.45 kN
Measurement Range(x or y axis)	500 lb	2.22 kN
Maximum Force(z axis)	1320 lb	5.87 kN
Maximum Force(x or y axis)	660 lb	2.94 kN
Maximum Moment(z axis)	14 ft-lb	18.98 N-m
Maximum Moment(x or y axis)	13 ft-lb	17.63 N-m
Broadband Resolution(z axis)	0.006 lb-rms	0.027 N-rms
Broadband Resolution(x or y axis)	0.002 lb-rms	0.0089 N-rms
Upper Frequency Limit	90 kHz	90 kHz
Low Frequency Response(-5 %)(z-axis)	0.01 Hz	0.01 Hz
Low Frequency Response(-5 %)(x or y axis)	0.001 Hz	0.001 Hz
Non-Linearity	≤ 1 % FS	≤ 1 % FS
Cross Talk(between x and y axis)	± 3 %	± 3 %
Cross Talk(between (x or y axis) and z axis)	± 5 %	± 5 %
Physical		
Preload	5000 lb	22.25 kN
Stiffness(z axis)	10 lb/μin	1.75 kN/μm
Stiffness(x or y axis)	4 lb/μin	0.7 kN/μm
Size (Height x Length x Width x Bolt Diameter x ID x Sensing Surface)	0.390 in x 1.075 in x 0.95 in x 0.205 in x 0.319 in x 0.680 in	9.90 mm x 27.3 mm x 24.1 mm x 5.21 mm x 8.10 mm x 17.27 mm
Weight	0.927 oz	26.27 gm
Housing Material	Stainless Steel	Stainless Steel
Sealing	Hermetic	Hermetic
Electrical Connector	4-Pin	4-Pin
Electrical Connection Position	Side	Side

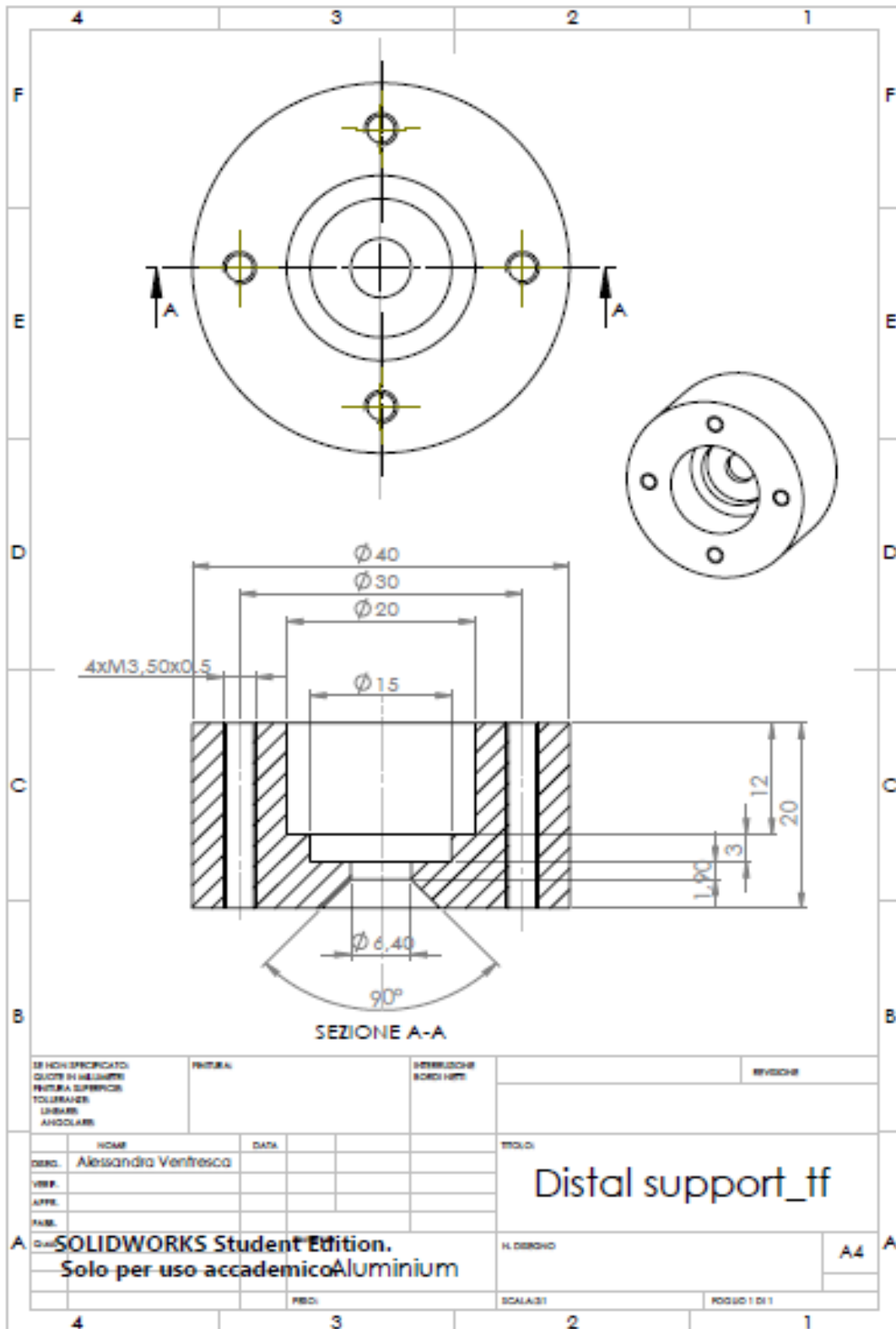


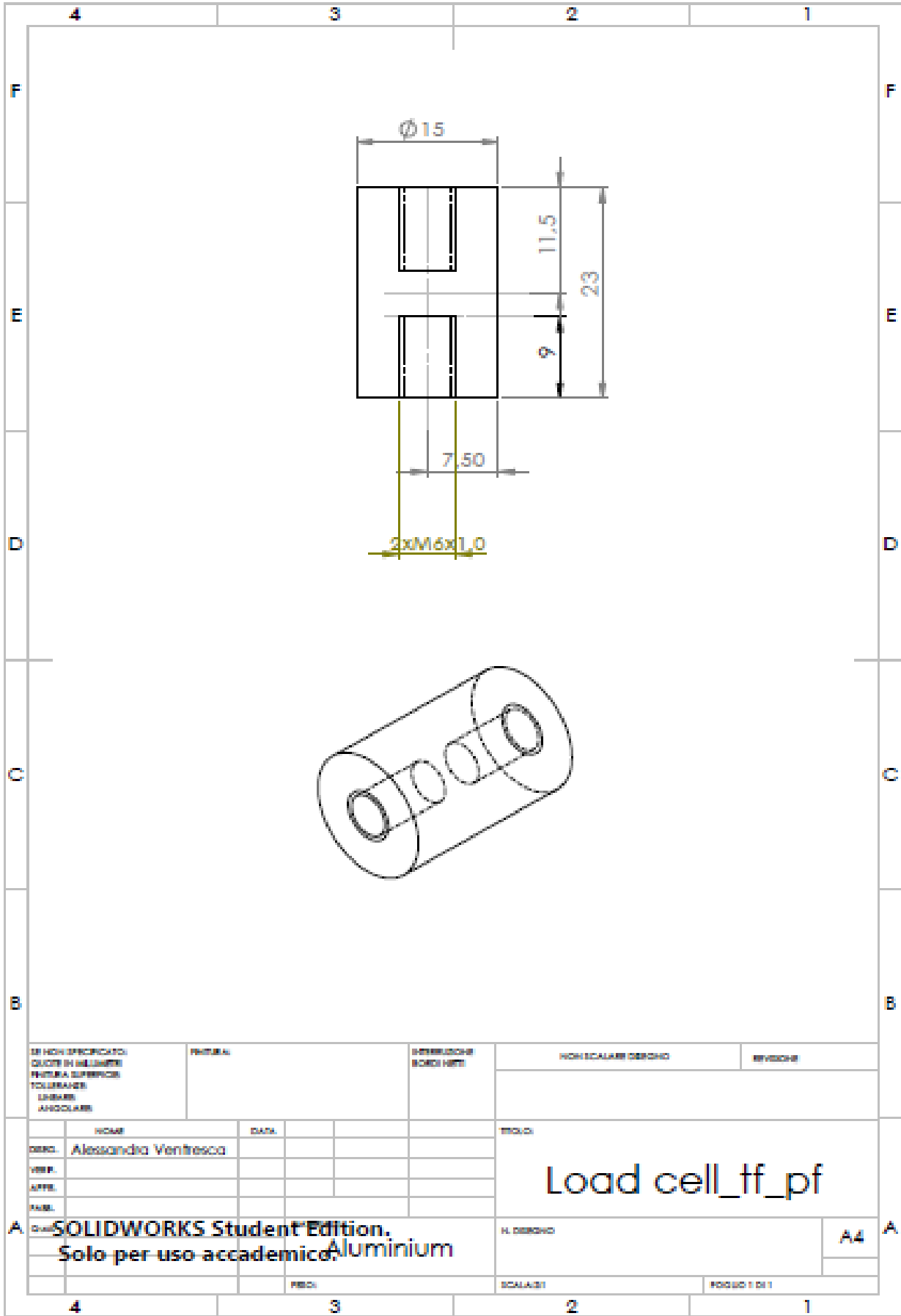
[5]
[3]
[3]

PCB PIEZOTRONICS™
FORCE / TORQUE DIVISION
3425 Walden Avenue, Depew, NY 14043

B - Technical Drawings

Instrumented Tibial tray





SE NON SPECIFICATO:
 QUOTE IN MILLESIMI
 FINITURA SUPERFICIE
 TOLLERANZE
 LINEARI
 ANGOLARI

FINITURA

INTERROGHI
 BORDI VERTI

NON SCALARE DISEGNO

REVISIONI

DESCR.	NOVITÀ	DATA	PRODOTTORE	PRODOTTORE
DESIGNER	Alessandra Ventresca			
VERIF.				
APPR.				
TRACC.				

TITOLO

Load cell_tf_pf

SOLIDWORKS Student Edition.
 Solo per uso accademico. Aluminium

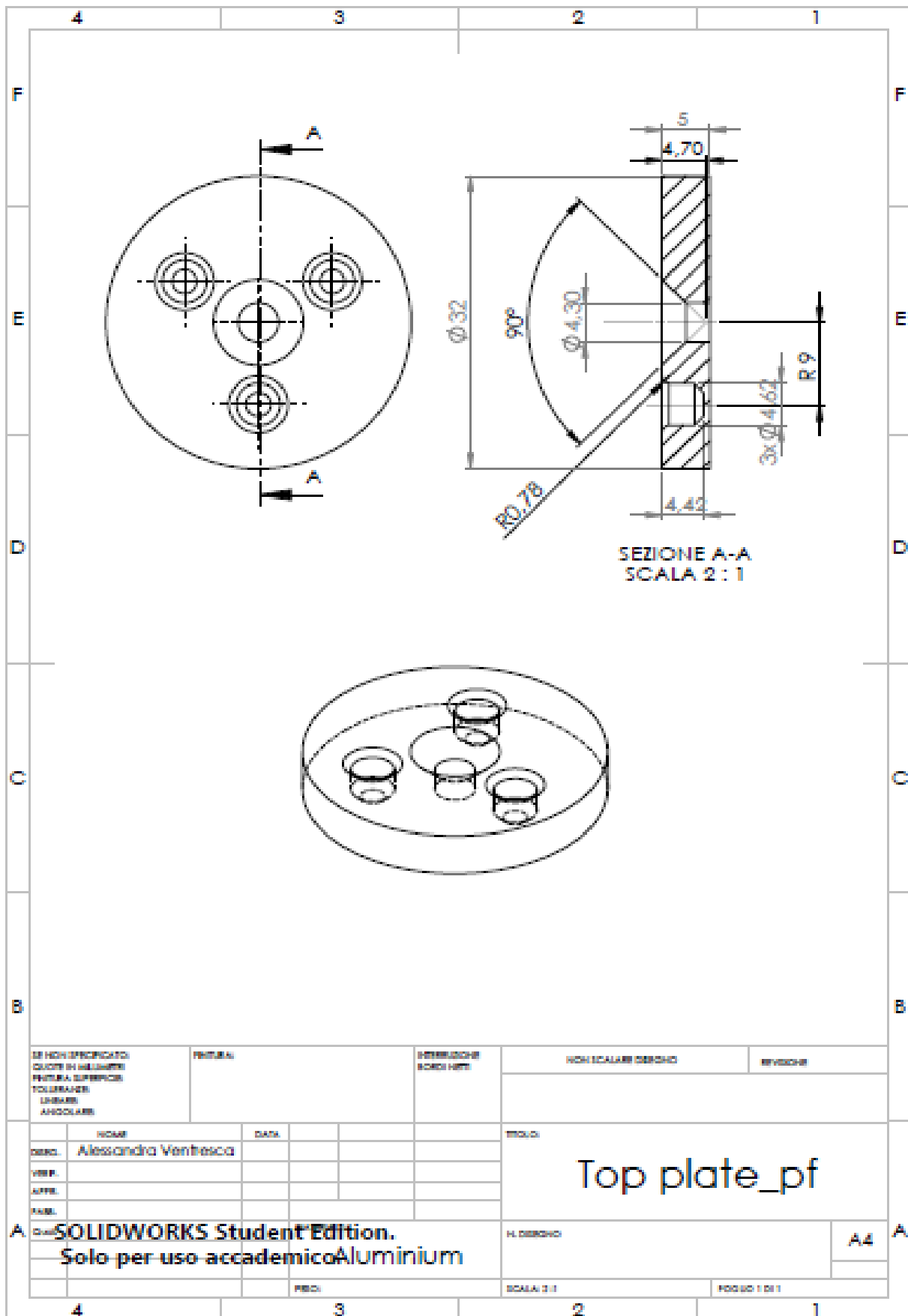
N. DISEGNO

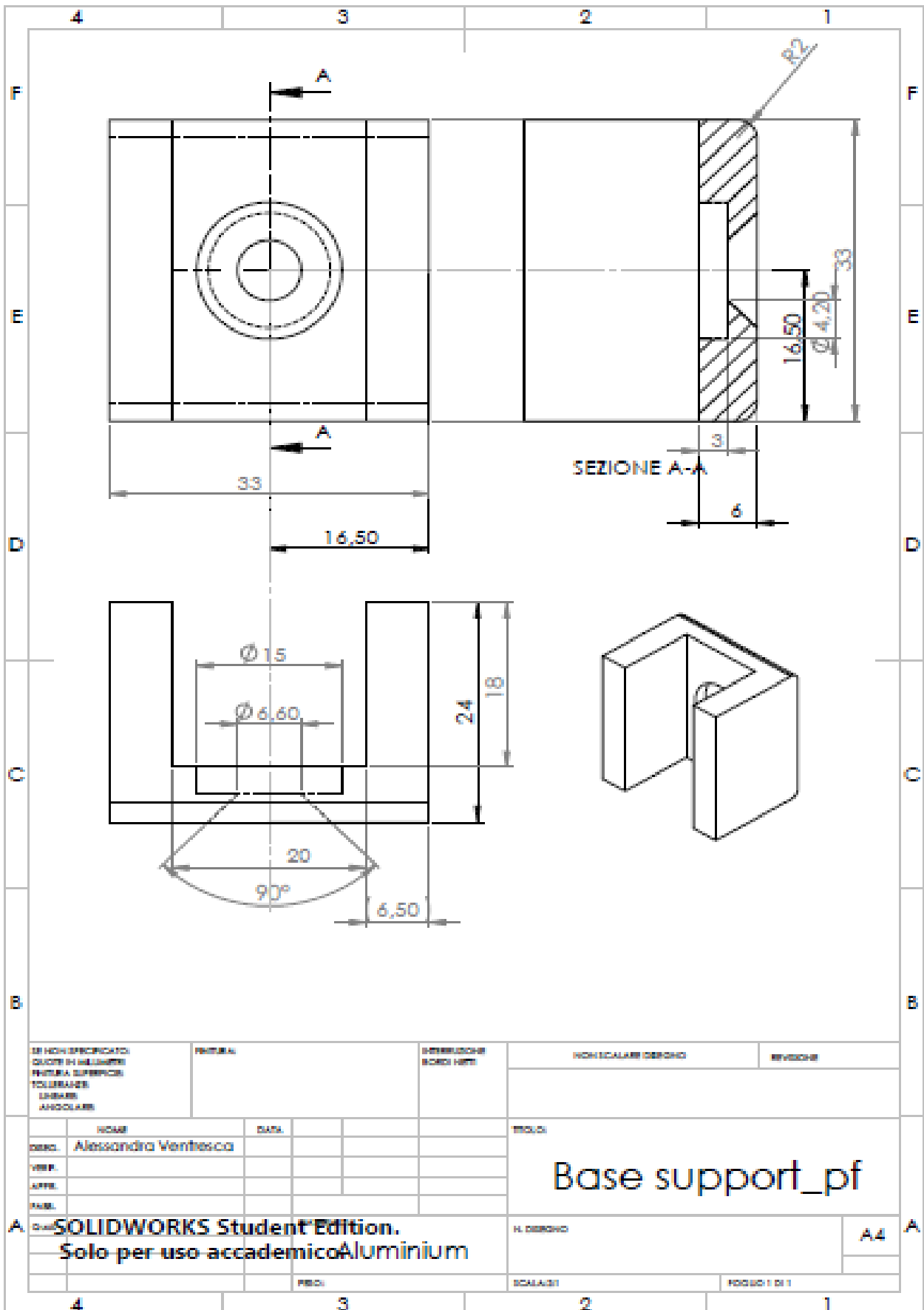
A4

PRODOTTORE

SCALE/IST

FOGGIO 1 DI 1





SE NON SPECIFICATO
 QUOTE IN MILLESIMI
 FINITRA SUPERFICIA
 TOLLERANZE
 LINEARI
 ANGOLARI

MATERIA

INTERROGARE
 BORDI VERTI

NON SCALARE DERIVATO

REVISIONE

COND.	NOOME	DATA		
DIR.	Alessandra Ventresca			
VIMP.				
APP.				
PRO.				

TITOLO
Base support_pf

A **SOLIDWORKS Student Edition.**
Solo per uso accademico Aluminium

N. DERIVATO
 A4

PROG.	SCALA: 1:1	Foglio 1 di 1
-------	------------	---------------

C – Strain gauges datasheets





Single element linear strain gauges

FOIL STRAIN GAUGE series "UF"

Compatible adhesive & Operational temperature
 CN : -20~+120°C
 NP-50 : -20~+150°C EB-2 : -20~+150°C







Operational temperature -20~+150°C
 Temperature compensation range +10~+100°C

GENERAL USE

Gauge pattern	Type	Gauge size		Backing		Resistance in Ω	
		L	W	L	W		
L : length W : width (Unit : mm)							
● Single-element (G.F. 2.1 approx.)  UFLA-1-350 (X3)	High gauge resistance Single-element	UFLA-1-350-11	1	1.6	4.6	3.0	350
 UFLA-2-350 (X3)		UFLA-2-350-11	2	1.9	6.1	3.5	350
 UFLA-3-350 (X3)		UFLA-3-350-11	3	1.6	7.2	3.0	350
 UFLA-5-350 (X3)		UFLA-5-350-11	5	1.8	9.4	3.8	350

45°/90° 3-element Rosette

GENERAL USE

Gauge pattern	Type	Gauge size		Backing		Resistance in Ω
		L	W	L	W	
● 45°/90° 3-element Rosette (G.F. 2.1 approx.)						
Stacked type						
 FRA-1	45°/90° 3-element Rosette, Stacked type	FRA-1-11	1	0.7	φ 4.5	120
 FRA-2		FRA-2-11	2	0.9	φ 7.0	120
 FRA-3		FRA-3-11	3	1.7	φ 11.0	120
 FRA-5		FRA-5-11	5	1.9	φ 12.0	120
 FRA-6		FRA-6-11	6	2.4	φ 14.0	120
 FRA-10		FRA-10-11	10	2.5	φ 17.0	120
		350 Ω	FRA-3-350-11 FRA-3-350-17 FRA-3-350-23	3	2	φ 11.0

D – LabView program

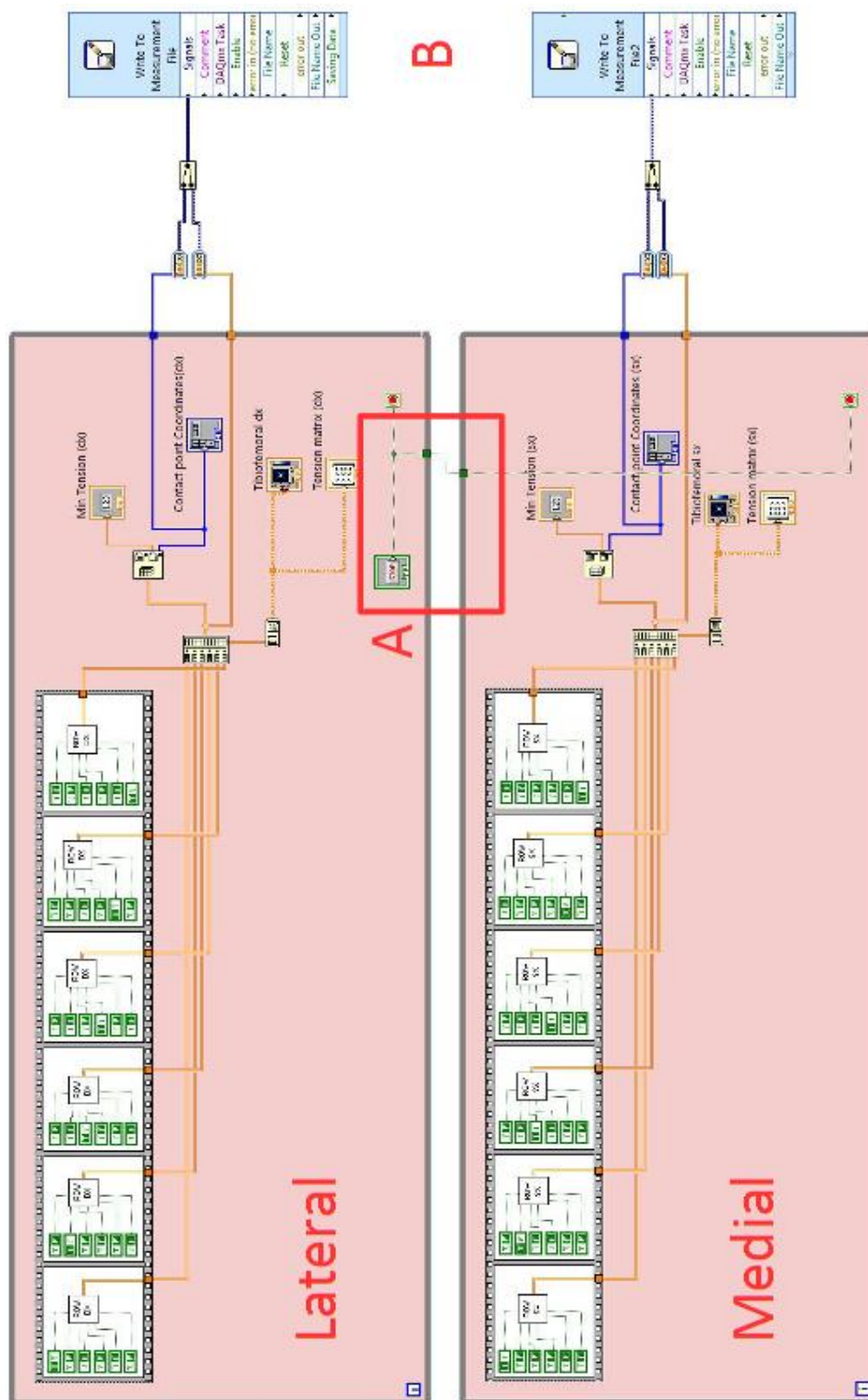


Fig. D 1: The LabView code is composed by two identical While loops (Function palette: Programming → Structures → While loop) for the medial and lateral sensor data acquisition. When the user stops the data acquisition through the stop button in the front panel (which is the same for both cycles to synchronize them (A)) the two acquisition matrix are stored in two different files. (B) (Function palette: Programming → File I/O → Write to Measurement file).

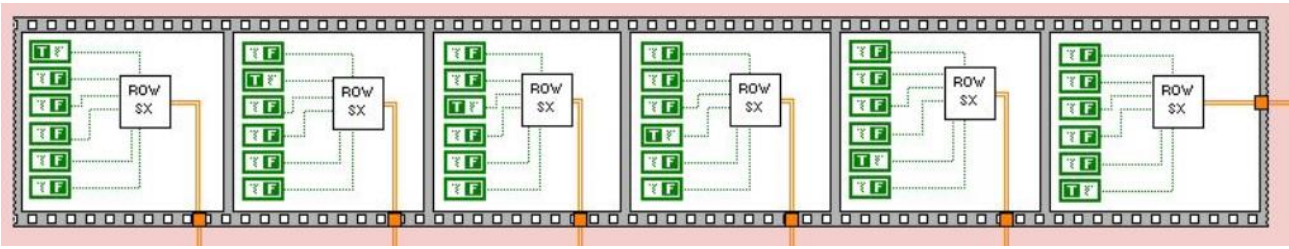


Fig. D 2: Each loop consists of a Flat Sequence (Function palette: Programming → Structures → Flat Sequence) with six frames, each containing a SubVI to capture the voltage outputs of a row of the sensor. This structure allows you to acquire the lines one after the other until the stop command by the user.

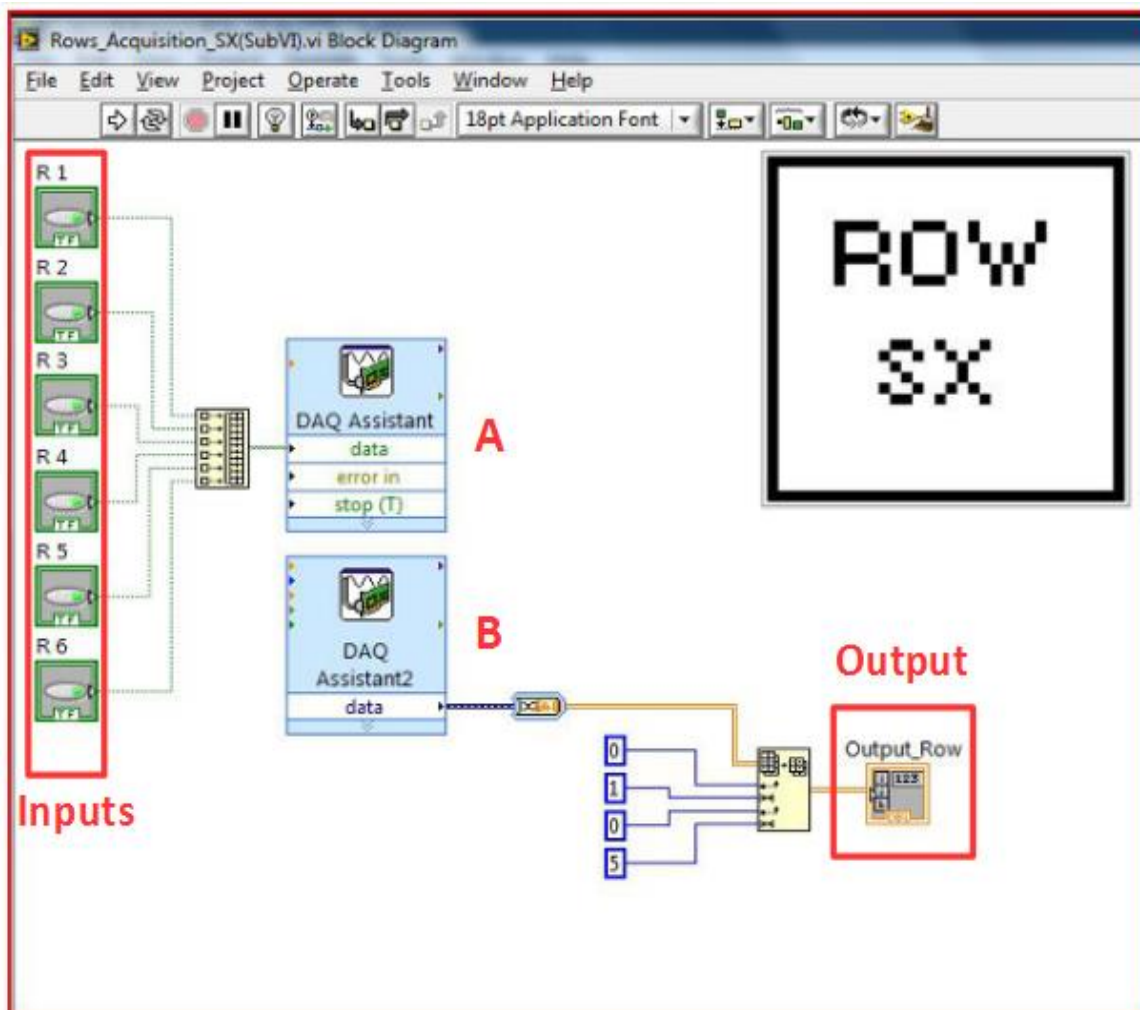


Fig. D 3: The inputs of the SubVI, set in an array (Function palette: Programming → Array → Build array) are six Boolean values, one per row ($R_i, i:1...6$). Each Boolean value is linked to a Digital Output virtual channel of the DAQ assistant A. Using DAQ assistant B, five voltage channels are acquired, one for each column of the sensor : the Output of SubVI is a five-element array and represents a row acquisition of the sensor (*Output_Row*).

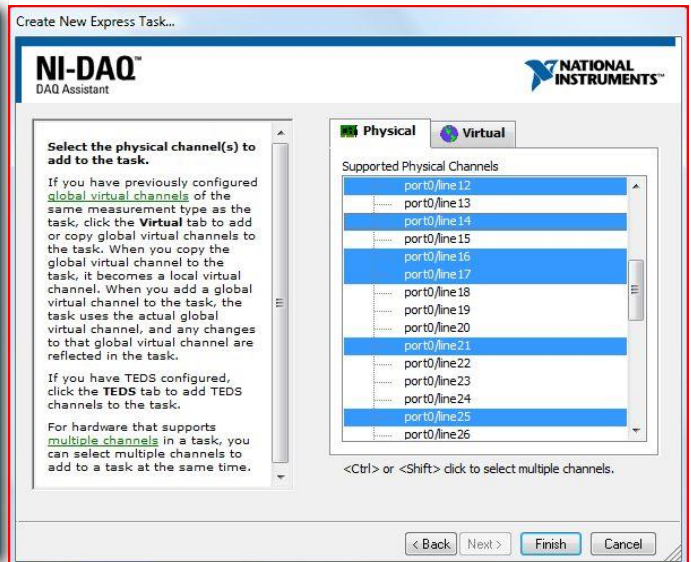


Fig. D 4: DAQ Assistant A: Digital output task with six virtual channels, one for each row. (Function palette: Express → DAQ Assistant → Generate Signal → Digital Output) . Each virtual channel corresponds to a physical channel of the NI PXI-6224. Only those rows of the sensor connected to a channel " true " will be connected.

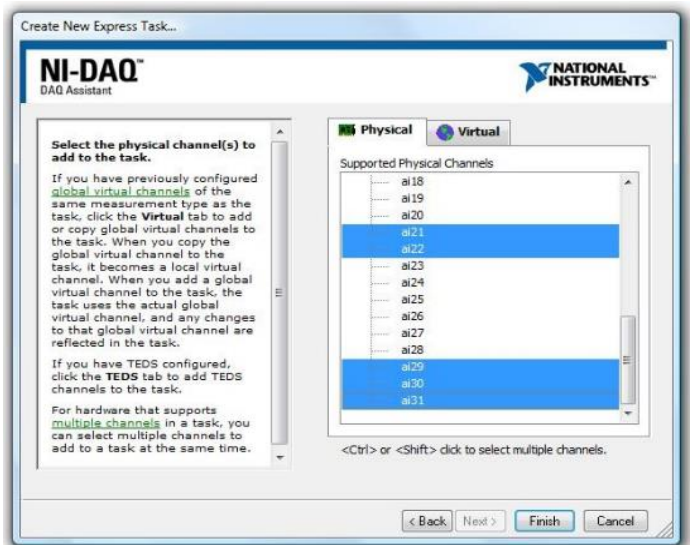


Fig. D 5: DAQ Assistant B: Analog Input task with five virtual channels, one for each Column. (Function palette: Express → DAQ Assistant → Acquire Signal → Analog Input) . Each virtual channel corresponds to a physical channel of the NI PXI-6224, wired to the column of the sensor.

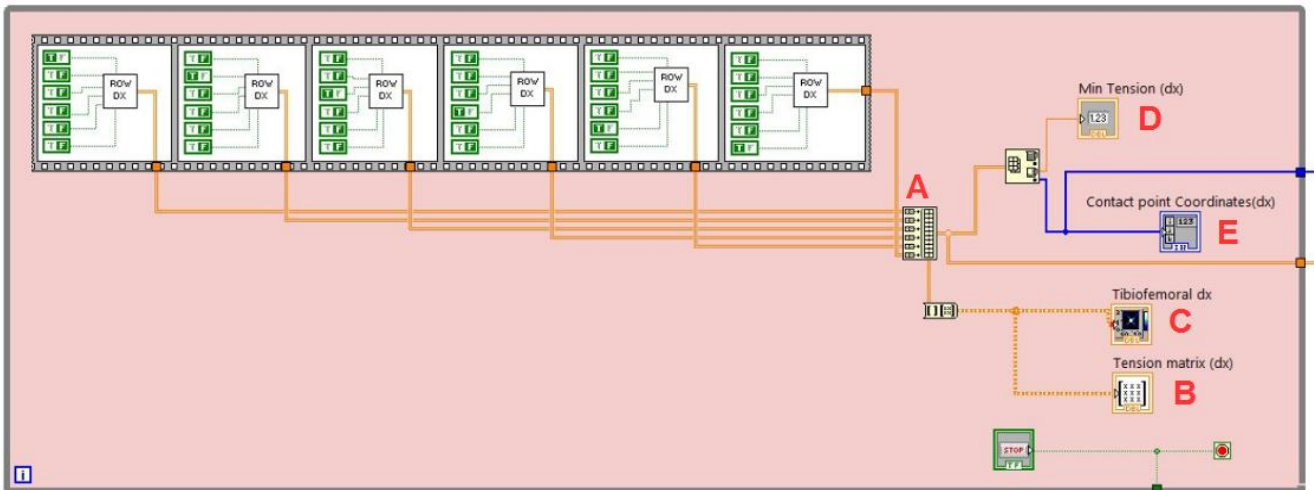


Fig. D 6: While loop of Lateral sensor. In each frame, only one line is "on". Output arrays are collected in a matrix (A), displayed on the front panel (B), also displayed on a 2-D chart (C). The minimum voltage is calculated (D), and its x-y-spatial coordinate (E) on the matrix (contact point).